applied sciences

MDPI

Review

Rationalizing Structural Hierarchy in the Design of Fuel Cell Electrode and Electrolyte Materials Derived from Metal-Organic Frameworks

Aniket Kumar [1], Prashant Purwar [2], Sanjiv Sonkaria [3,*] and Varsha Khare [3,*]

[1] School of Materials Science and Engineering, Chonnam National University, Gwangju 61186, Korea; aniket.cnukorea@gmail.com
[2] Department of Mechanical and Aerospace Engineering, Seoul National University, Seoul 08826, Korea; ppurwar@snu.ac.kr
[3] Nanosystems Research Institute, Seoul National University, Seoul 08826, Korea
* Correspondence: ssonkaria64@snu.ac.kr (S.S.); khare@snu.ac.kr (V.K.)

Abstract: Metal-organic frameworks (MOFs) are arguably a class of highly tuneable polymer-based materials with wide applicability. The arrangement of chemical components and the bonds they form through specific chemical bond associations are critical determining factors in their functionality. In particular, crystalline porous materials continue to inspire their development and advancement towards sustainable and renewable materials for clean energy conversion and storage. An important area of development is the application of MOFs in proton-exchange membrane fuel cells (PEMFCs) and are attractive for efficient low-temperature energy conversion. The practical implementation of fuel cells, however, is faced by performance challenges. To address some of the technical issues, a more critical consideration of key problems is now driving a conceptualised approach to advance the application of PEMFCs. Central to this idea is the emerging field MOF-based systems, which are currently being adopted and proving to be a more efficient and durable means of creating electrodes and electrolytes for proton-exchange membrane fuel cells. This review proposes to discuss some of the key advancements in the modification of PEMs and electrodes, which primarily use functionally important MOFs. Further, we propose to correlate MOF-based PEMFC design and the deeper correlation with performance by comparing proton conductivities and catalytic activities for selected works.

Keywords: polymer electrolyte membrane; fuel cells; metal-organic frameworks (MOFs); electrode; electrolyte; proton conductivity; structural hierarchy

Citation: Kumar, A.; Purwar, P.; Sonkaria, S.; Khare, V. Rationalizing Structural Hierarchy in the Design of Fuel Cell Electrode and Electrolyte Materials Derived from Metal-Organic Frameworks. *Appl. Sci.* **2022**, *12*, 6659. https://doi.org/10.3390/app12136659

Academic Editor: Daniel Villanueva Torres

Received: 18 May 2022
Accepted: 27 June 2022
Published: 30 June 2022

1. Introduction

Polymer electrolyte membrane fuel cells (PEMFCs) have the potential to succeed as a breakthrough technology through the utilization of miniaturized materials at the nanoscale for the efficient conversion of chemical to electrical energy [1–4] since its conception decades ago [5]. Fuel-cell performance is inherently determined from the properties of the membrane electrode assembly (MEA) efficiency, which principally generates electrical energy from a chemical source. Architecturally, MEAs generally comprise a catalyst layer on opposing surfaces, a polymer electrolyte membrane (PEM) layer, and a gas diffusion layer located in the interior segment. The catalyst layer in the MEA is characterised by two electrochemical reactions that are principally related to their function, namely the hydrogen oxidation reaction (HOR) and the oxygen reduction reaction (ORR) [6], which direct the conversion of chemical energy to electrical energy at the anode and cathode, respectively [7,8]. Further, the PEM layer functions as a proton conductor, permitting the mobility of protons from the anode to the cathode. Nevertheless, activity loss of the catalyst layer and conductivity loss of PEM pose significant performance problems in the long run [9,10]. To advance Fuel-cell

technology on larger scales, it becomes necessary to formularize catalysts and electrically conductive materials with highly efficient and durable electrochemical characteristics. It is highly desirable for these materials to have appropriate compositions and nanostructures to solve these problems. Hence, Fuel-cell technology requiring high efficiency with durability and rationalizing the design of functionally meaningful materials to address the issues discussed above is of paramount importance.

Metal-organic frameworks (MOFs) have been developed to assist the process of efficient energy conversion and storage systems. MOFs are porous polymeric materials composed of self-assembled ligands forming organic bridges (dicarboxylic acid, tricarboxylic acid, tetracarboxylic acid, and imidazolate) in combination with metal ions that result in the opening of porous crystalline frameworks as shown in Figure 1. The MOF hierarchy generally conform to porous, architectural and compositional structural types. MOF hierarchical pores display multiscale porosity in the pattern of the framework, including micro-porosity, meso-porosity, and macro-porosity, a feature that was summarized in recent years [11–13]. Depending on how they are constructed, these pores can be intrinsically arranged, or they can be post-synthetically etched by using a template [14,15]. In addition to the facile tunability of pore sizes, the ability to change reaction pathways, and the improvement of diffusion kinetics to better reach active sites, the architectural configuration of porous MOFs provide significant avenues for introducing structural modifications by synthetic means, thus advancing hierarchical properties whilst retaining their porosity [16,17]. From a functional perspective, the design of hierarchical geometries in the MOF assembly is recognizably critical for electrodes and electrolytes in Fuel-cell operation [18]. For example, hierarchical MOF superstructure design features have proved strategic for enhancing the packing density of frameworks and fabricating multi-assembled geometries for applications including transportation and catalysis [19]. The dynamics of nucleation and growth may be tuned to generate superior MOF structures with a unique morphology. Hence, the physical morphological order of MOF cages can be synthetically directed to embody pores as large as 9.8 nm by altering the organic and metal components with surface areas typically ranging between 1000 and 10,000 m^2/g [20–22]. The adaptable nature of metal nodes with the array of organic linker combinations that can be generated under controlled conditions can provide key insights into achieving highly ordered and tuneable MOFs possessing unique compositional and structural advantages over conventional materials (Figure 2).

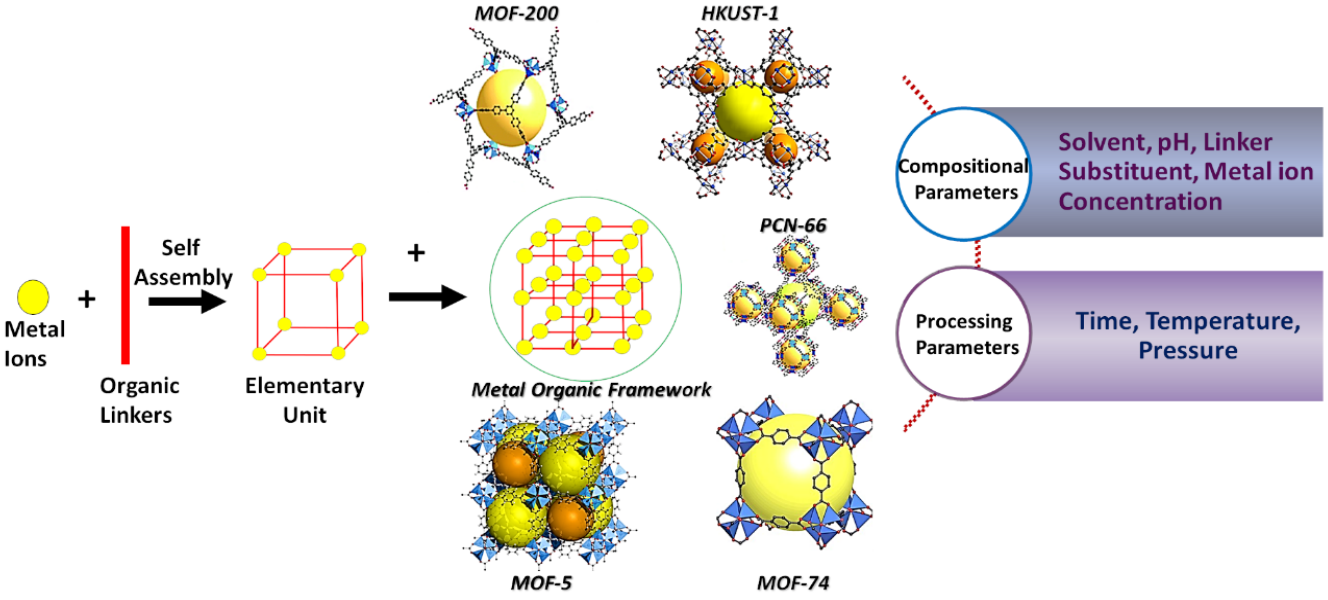

Figure 1. Illustrating the formation of MOFs and factors that affect their synthesis.

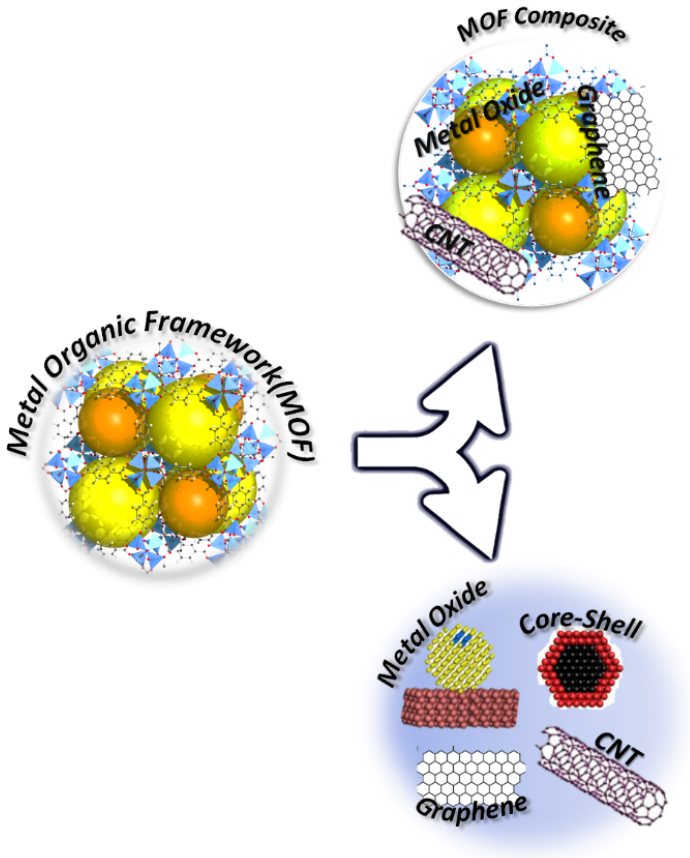

Figure 2. The diagram shows the dependence of MOF composites and their derivatives on the base MOF structure.

PEMFC technology can be made more efficient by using MOF materials that possess appropriate physical and chemical properties. The most commercially studied and applied proton-exchange membranes are composition-based nafion membranes. In the presence of water in the range of 20~80 °C, the proton conductivity of nafion is achievable up to 10^{-2} S cm^{-1} [23–25]. Although nafion membranes and their derivative membranes have been widely investigated, they have limited use in fuel cells owing to the complex preparation process and high production costs, which become significant and commercially demanding at temperatures exceeding 80 °C and below 0 °C as mirrored by a considerable fall in conductivity [9,26,27]. Hence, the requirements for high proton conductivity (>100 S cm^{-1}) and a broad temperature range (25~300 °C) considerably reduce its commercial value, necessitating a greater need for alternative proton-exchange membranes, which are less demanding in an industrial context [28]. MOFs are viewed as attractive replacement materials that demonstrate a wider physical and chemical property range, in conjunction with mechanical properties for durability. Investigations have shown that the coordination skeleton itself plays a leading role in delivering protons as a carrier [29,30]. However, a significant disadvantage is the insufficient conductivity of MOFs due to the grain boundaries, which restrict proton migration, but the hybridization of MOFs using acid groups (-COOH, -HSO_3, -PO_3H_2, etc.) offers an efficient strategy for resolving this problem [31–33].

Additionally, Fuel-cell efficiency is also dependent on the activity of the oxygen reduction reaction, which is classified among the essential half-reactions [34–37]. For the development of durable fuel cells, the search for electrocatalysts with superior efficiencies is therefore a significant hurdle. More recently, MOFs have been attractive for ORR applications [38–40] where the use of metal ions or clusters and organic connectors can aid the development of advanced catalysts. The porous structure of MOF electrocatalysts

facilitates mass transfer in electrochemical reactions, and as a result of the uniform distribution of metal throughout the MOF precursors, the active sites of the catalyst are efficiently utilized [41–44].

The purpose of the present review is to discuss the recent developments of the PEMFC electrode layer and electrolyte, highlighting the relevance to MOFs and their structures, modification and impact in advancing the next generation of PEMFC-based technologies. Future research directions and perspectives are also highlighted in Figure 3.

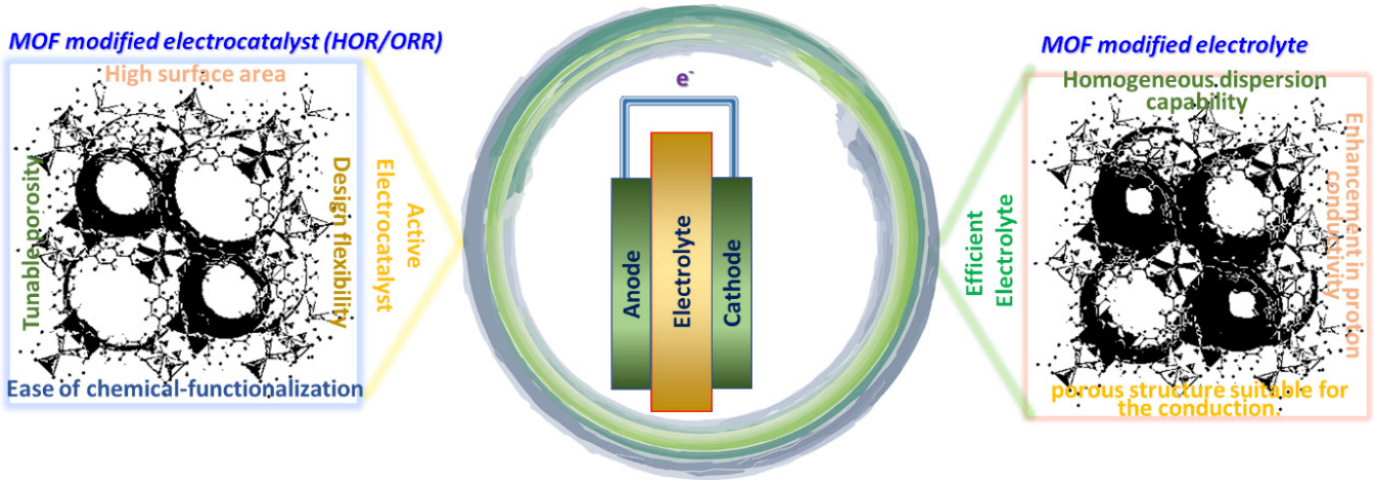

Figure 3. The scheme showing the criteria for selection of MOF for electrocatalyst and electrolyte modification for PEMFCs.

2. MOFs for Fuel-Cell Applications

2.1. MOFs as Electrode Application

The potential for supplying sustainable clean energy for Fuel-cell development through devices with capabilities to both store and deliver energy upon demand is accelerating efforts to engineer desirable MOF structures. However, these devices still seek technological improvement as usable electrocatalysts for the electrochemical reduction of oxygen as the base reaction (ORR) [45–47]. The durability and catalytic activity of electrocatalysts is pivotal for the long-term performance of the Fuel-cell system. Cost limitations combined with the precious metal shortage is a huge barrier to the commercialization of fuel despite their relatively low overpotential. However, the efficient usage of particles in nanoscale architectures provides a route for the expedition of metal sites at the surface and their dispersion in abundancy. There is a high potential for developing fuel cells in the future with these materials, especially those incorporating single-atom catalysts [48,49]. As has been established by the in-depth characterization of these species and theoretical studies, it has been demonstrated that the M-Nx type of single-atom catalyst (SAC) shows functional importance in the ORR/OER reactions in H_2/O_2 fuel cells [40,50]. It has been identified that a MOF template synthesis method is a promising way of achieving the controlled synthesis of SACs through the pyrolysis of precursors. In addition, those nanostructures that emerge from MOF-derived SACs have excellent active-site support and excellent dispersion properties when applied to electrocatalytic processes. High absorbent properties that persist and are likely better controlled in self-removable supports deliver porous, hollow, structurally defined cavities [51–54]. According to the results of our study, MOF-designed electrocatalysts for fuel cells are capable of improving their working durability and have the potential to replace precious metals as costly conventional materials. The performances of known metal catalysts are summarized in Table 1.

Table 1. Performances of MOF-based electrode materials in superior Fuel-cell devices.

Catalyst	MOF	Devices	Voltage (V)	Current Density ($mAcm^{-2}$)	Power Density ($mWcm^{-2}$)	Cycling Life
Fe-N-C [55]	Fe-ZIF-8	PEMFC	0.6 V	1650	1141	-
Fe-SAs/NPS-HC [56]	ZIF-8/Fe@PZS	H_2/O_2 fuel cell	0.8 V	50	333	-
Ferrocene [57]	ZIF-8	PEMFC	0.7 V	1100	775	32.2% (10 h)
C-FeHZ8@g-C_3N_4-950 [58]	Fe-ZIF-8@g-C_3N_4	PEMFC	0.8 V	133	628	48.7% (8 h)
Fe-N-C [59]	ZIF-8	PEMFC	0.7	1050	690	42% (50 h)
FeN_4/HOPC-c-1000 [60]	Fe-ZIF-8	PEMFC	0.6 V	690	420	53% (100 h)
Fe-Fe_3C [35]	ZIF-8	H_2-O_2 Fuel Cell	0.8 V	100	760	-
20 Mn-NC [61]	Mn-ZIF-8	PEMFC	0.6 V	350	460	>1000 h
20-Co-NC-1100 [62]	Co-ZIF-8	H_2/O_2 fuel cell	0.7 V	-	560	-
C-FeZIF-8@g-C_3N_4 [63]	Fe-ZIF-8	PEMFC	0.8 V	1000	481	82% (667 h)
Co-N-C@F127 [64]	Co-ZIF-8	H_2/O_2 fuel cell	>0.7 V	30	870	100 h
Fe-ZIF/CN-UC [65]	Fe-ZIF-8	H_2/O_2 fuel cell	0.2 V	2000	484	-
H-Fe-N_x-C [66]	ZIF-8@Fe-TA	PEMFC	0.43 V	1550	655	30 h
H-Co-N_x-C [66]	ZIF-8@Co-TA	PEMFC	0.43 V	103	457	30 h
H-FeCo-N_x-C [66]	ZIF-8@FeCo-TA	PEMFC	0.43 V	104	459	30 h
FeNi-N_6 [67]	ZIF-8	PEMFC	0.8 V	-	216	>5000 cycles
Fe-Fe_3C@Fe-N-C [35]	MIL-100/ZIF-8	PEMFC	0.8 V	100	760	-
GNPCSs-800 [68]	ZIF-8/GO	DMFC	0.71 V	-	33.8	94% (~8 h)
GO-MOF [69]	Cu-MOF	PEMFC	0.6 V	-	110.5	-
Fe-N-C-10/1-950 [70]	NH2-MIL-88B/ZIF-8	PEMFC	0.6 V	1240	770	-
PtCu@NCC [71]	ZIF-8	DFAFC	0.8 V	400	121	71% (40 h)
MOF-800 [72]	Cu-bipy-BTC	MFC	0.588 V	-	326	>30 days

2.1.1. H_2/O_2 Fuel Cells

The past few years have witnessed H_2/O_2 fuel cells gaining increasing popularity as a result of their high efficiency and environmental friendliness. However, a potential problem is associated with the slow kinetics of the ORR [73,74] that can be a hindrance for practical applications. In order to commercialize ORR technologies in the future, it is vital to develop efficient catalysts. A range of studies reported over the past few years have focused on SACs to address durability without impeding the atomic utilization of the catalyst. MOF-derived nanomaterials have also been deliberated for their potential role as functionally viable substitutes for platinum, which is a highly expensive metal in consideration of its excellent catalytic activity [49].

It has been demonstrated by a theoretical study that M-N_x is the most catalytically active species in the ORR [75,76]. The subjection of Fe-doped ZIF-8 to pyrolysis as a straightforward methodology for synthesizing Fe-N-C electrocatalysts for membrane fuel cells based on the principle of proton exchange (PEMFCs) has been suggested, which takes advantage of less expensive approaches without diminishing the superior catalytic properties of Fe. As a result of its atomic dispersion, Fe-N_4 functions as the active molecule for a highly efficient and stable acidic PEMFC. There is widespread use of MOFs for controlling the morphology and atom distribution of the desired products in MNC catalysts by using them as sacrificing templates. They have been effectively used to fabricate individual or unaccompanied Fe atomic sites on an N, P, and S co-doped carbon polyhedron with empty cavities (denoted as Fe-SAs/NPS-HC) using the ZIF-8/Fe@PZS method (P_{ZS} = poly(cyclo-triphospazene-co-4,4′-sulfonyldiphenol)) in a pyrolysis experiment at 900 °C in Ar [56]. In order to successfully synthesize highly ordered FeN_4-doped struc-

tures on a porous carbon (FeN_4/HOPC-C-1000) skeleton, Qiao et al. [60] carbonized the MOF Fe-ZIF-8 at 1000 °C. FeN_4/HOPC-c-1000 using a bimetallism mechanism demonstrating a current density of 0.69 A cm^{-2} at 0.6 V, which exceeds current expectations up to 0.5 A cm^{-2} for FeN_4/C, and a power density of 0.42 W cm^{-2} at 0.57 V (0.35 W cm^{-2} for FeN_4/C). Aside from this, the catalyst also exhibited impressive durability when annealed at 0.55 and 0.7 V. These results suggest an atomically dispersed FeN_4 with catalytic centres that exhibit a porous structure when annealed at optimum temperatures. An alternative method of the binary ligand strategy aimed at a higher surface area was also presented by using 2-methylimidazole (mIm) and 2-undecylimidazole (uIm) as ligands. This study has offered new methods for the controlled preparation for electrocatalysts of the Fe-N-C type [60,77] (Figure 4).

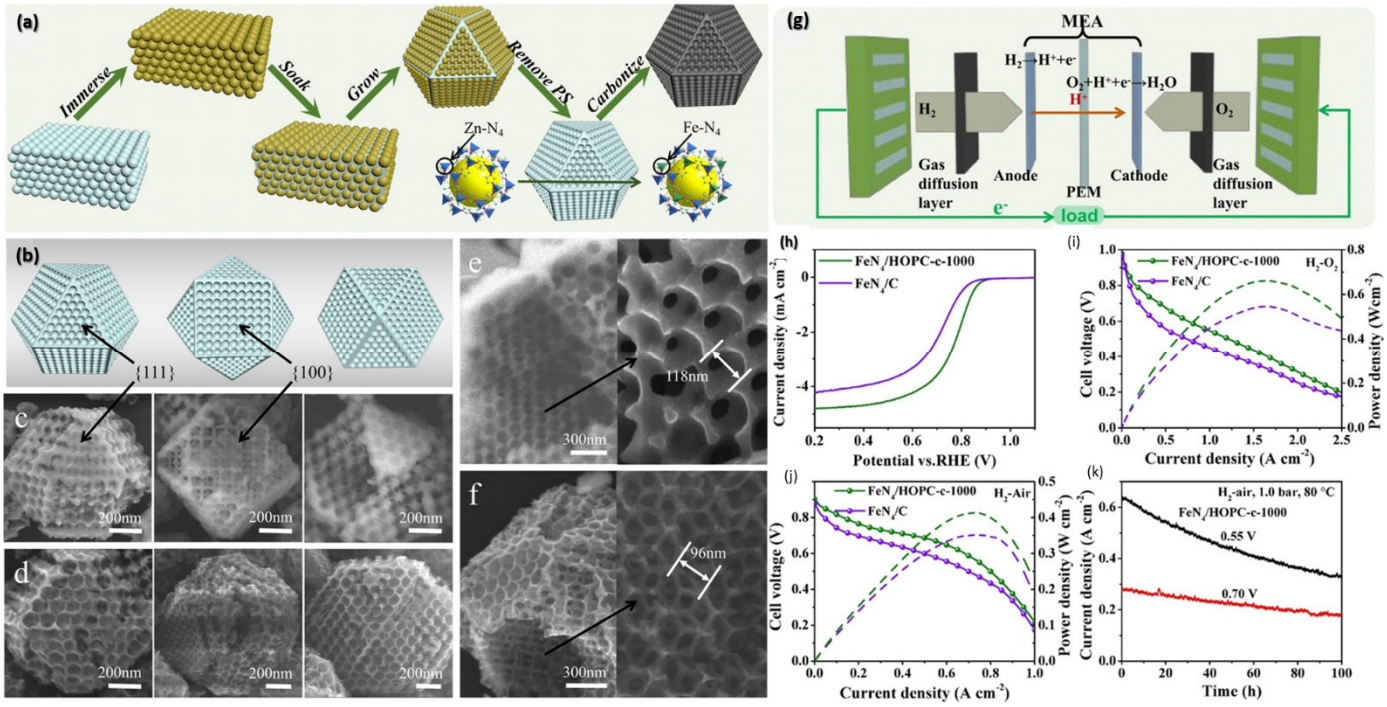

Figure 4. (**a**) The schematic showing the FeN_x/HOPC-c-1000 synthesis steps; (**b**) model of the OMS-Fe-ZIF-8 seen from different crystallographic orientations; (**c**,**d**) SEM images of the OMS-Fe-ZIF-8 showing growth along multiple crystallographic planes; (**e**) SEM image and details about the inner geometry of a broken crystal of OMS-Fe-Z(F-8); (**f**) the SEM image shows the internal structure of one of the FeN_4/HOPC-c-1000 particles that has broken in two; (**g**) illustration of the PEMFC Fuel-cell assembly; (**h**) LSV curves of FeN_4/HOPC-c-1000 and FeN_4/C in 0.5 M H_2SO_4, with a scan rate of 10 mVs^{-1} in 0.5 M H_2SO_4 under unsaturated O_2; (**i**,**j**) polarization and power−density measurements carried out using a cathode catalyst of H_2-O_2 and a catalyst of FeN_4/HOPC-c-1000 at 1 bar and (**k**) a constant-potential test to determine Fuel-cell durability [60].

As a result of their higher stability and remarkable catalytic activity, other transition-metal-based catalysts have also been examined in H_2/O_2 fuel cells. The Fenton reactions (Fe^{2+} + H_2O_2) used by Fe-N-C catalysts were addressed by developing a Mn-N-C type SAC with MnN_4 species being chemically distributed through the calcination of Mn-doped ZIF-8 precursors in an acid environment [61]. In order to achieve optimal performance, the proportion of Mn and Zn was adjusted to yield 200 Mn-NC SACs having a life of 1000 h at 0.7 V. Cobalt is another multivalent metal that shows excellent electrocatalytic participation, so the Co-N-C type SACs have also been investigated as catalysts devoid of Fe for H_2/O_2 fuel cells [78]. By a similar calcination procedure, they were also able to synthesize the Co-N-C catalyst, which behaved similar to the Fe-N-C catalysts and displayed a similar performance to that of the Fe-N-C catalysts owing to the well-distributed CoN_4 operating

sites, which were afforded by the MOF template [43,62]. In spite of the encouraging catalytic activity of catalysts containing Co-N-C, the presence of agglomerated regions of Co might reduce the intrinsic capabilities of Co and N, which are atomically dispersed within the ZIF-8 precursor, forming a Co-N-C@F127 catalyst after a composition of Pluronic F127 block copolymer is utilized as a surface-active agent to confine the Co aggregates and collapse the porous structure. As predicted by density functional theory calculations, CoN_{2+2} active sites, with their relatively low energy of activation 0.69 eV as compared with CoN_4, were capable of catalysing the $4e^-$ ORR process [64,79]. The problem of functional deficiency from high voltage exposure must, however, be addressed in more detailed studies. Due to the success of separating sites singularly as applied to M-N-C electrocatalysts in H_2/O_2 fuel cells, great efforts have been made to combine different active metal centres for fuel cells. An N-doped carbon matrix was synthesized by Wang et al. [80] to be a Pt-free catalyst that consists of Fe and Co automatically dispersed within the matrix (Figure 5a). There is encouraging evidence to suggest that the existence of double metal sites are necessary for the initiation of the O-O bonds from passive to active forms and the engagement of the $4e^-$ ORR processes, as the hydrogen–oxygen Fuel-cell experiments and hydrogen-air Fuel-cell experiments clearly demonstrate. It was determined that the proposed (Fe,Co)/N-C catalyst performs better in both the H_2/O_2 and H_2/air conditions than most reported Pt-free catalysts. This shows that the dual metal sites have a high stability in the Fuel-cell test, suggesting that they have the potential to be produced commercially (Figure 5b,c) [80].

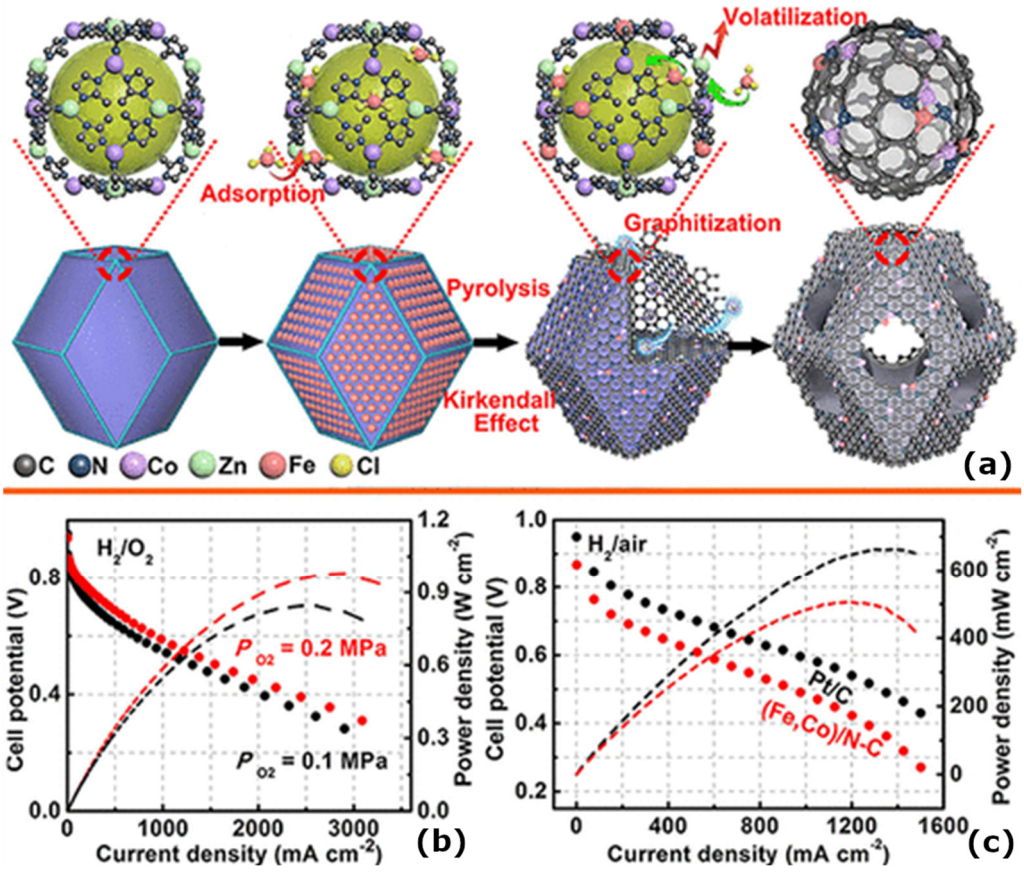

Figure 5. (**a**) Schematic illustration for the preparation of (Fe,Co)/N-C; (**b**) H_2/O_2 Fuel-cell polarization plots. Cathode: ~0.77 mg cm^{-2} of (Fe,Co)/N-C; 100% RH; O_2, 0.1 and 0.2 MPa partial pressures. Anode: 0.1 mg Pt cm^{-2} Pt/C; 100% RH; H_2, 0.1 MPa partial pressure; cell 353 K; 25 cm^2 electrode area and (**c**) polarization plots for hydrogen/air fuel cells. The cathode has a partial pressure of 0.2 MPa; the catalyst is (Fe,Co)/N-C; 100 percent relative humidity is used. H_2 at 0.1 MPa partial pressure; 100% RH; 0.1 mgPt cm^{-2} Pt/C at anode. Cell 353 K; electrode surface 25 cm^2 [80].

In order to gain insight from the exchanges between different metal sites in key locations of the electrocatalyst, Ying et al. created SACs with numerous operational site locations (Fe, Co, Ni) in order to explore the specific properties of the electrocatalysts [66]. However, despite the presence of multifaceted metal sites on the multiple metal catalysts, the open circuit voltage suffered severe decay, requiring improvements in both the ratio of the different metal sites as well as in the structural engineering. To avoid metal accumulation through the provision of additional hierarchical pores, liquid SiO_2 was supplemented in the reacting system with ZIF-8, FePc and NiPc (Pc = phthalocyanine) [67]. When FeNi-N_6 was prepared with four N atoms coordinated with the metal atoms, there were fewer H_2O_2 yields and the four-electron process resulted in better catalytic performance and longer operating life. In the majority of active sites in electrocatalysis, Fe dominated while Ni enhanced the cycling stability [43]. It can be concluded that active sites are very important for electrocatalysis [67].

With the application of the above catalysis design principles, organic fuel cells can achieve rapid ORR kinetics and can also benefit from a longer cycling life. The objective is to improve the shielding of functioning sites and increase catalysis. Zhang et al. designed Cu, N-incorporated carbon-based materials as catalysts. They prepared them by pyrolyzing Cu-bipy-BTC, where bipy is 2,2′-bipyridine and BTC is 1,3,5-tricarboxylate. In its present form, this catalyst consists of a copper–bispyridine–bistricarboxylate alloy that was burned at 800 °C at high pressure to produce a sufficiently high number active sites, in particular C-N and Cu-N_x. This catalyst was also fabricated to be porous (MOF-800) and has a high surface exposure [72].

There is an urgent need for the further development of efficient catalysts due to the slow ORR reaction kinetics that severely slow down the performance of H_2/O_2 fuel cells. To effectively design MOF-based catalysts, it is necessary to consider ligands that contain N, such as 2-methylimidazole, as well as metals such as Fe, Co, and Mn, all of which have remarkably high catalytic activity for ORRs. In addition to good performance, morphology control is also an important aspect, since metal-centre electrodes are able to efficiently utilize the atoms due to their well-dispersed nature. An additional way of improving catalytic capacity is to take advantage of the synergistic effects between the active sites. The problem with finding the right catalyst for H_2/O_2 fuel cells remains a significant challenge, as all of the above conditions must be met at the same time.

2.1.2. Organic Fuel Cells

A Pt-free electrocatalyst has been developed based upon the M-N_x active sites that have already been broadly employed as catalysts for accelerating the ORR process in H_2/O_2 fuel cells. They have proven to be effective at accelerating the ORR process in hydrocarbon fuel cells. A process of oxidizing the organic fuel also encompasses the ORR, and the result is the transformation of chemical energy into its electrical and thermal forms. An analogy can also be made with the oxidation of hydrogen and oxygen fuel cells. The use of methanol fuel cells for high energy density is a good example of a fuel cell that can be used for a variety of organic fuels. In order to ensure that the ORR catalysts used in direct methanol fuel cells (DMFCs) have good methanol tolerance, durability, and stability, the need to design them with good ORR tolerance and structure is paramount [81,82]. The use of ZIF-8 on graphene oxide after being subjected to thermal treatment at 800 °C reported the fabrication of a carbon porous framework that utilized a graphene-based layered material (GNPCSs-800) [83]. Furthermore, this Pt/C catalyst exhibits significant performance improvements over other conventional Pt/C catalysts in terms of open circuit voltage as well as methanol tolerance. This is partially due to the synergy linking the surface modification of graphene to accommodate the N-doped porous carbon layers.

Furthermore, carbon materials generally have the ability to perform as catalysts in fuel cells and are extremely resistant to organic media. As a way to exploit the excellent catalytic capability of Cu centres, Jahan et al. designed and fabricated a composite containing GO and Cu-structured MOFs in order to additionally enhance their ORR/OER activity [84]. They

were also able to integrate the sealing and electrical properties of GO into the composite. In a polymer electrolyte membrane fuel cell, MOF composite catalysts produced power densities that were comparable to those of platinum-based catalysts [43]. The NH_2-MIL-88B and ZIF-8 iron and carbon sources, respectively, were utilized in order to make a structure that was shown to resemble a bamboo structure mimicked by a carbon nanotube complex with Fe-positioned active-site nodes. A metal catalyst, which is open-source, was tested in the polymer electrolyte membrane fuel cell and showed excellent results when used as a catalyst [70].

There is no doubt that when designing MOF-based electrocatalysts, it is very critical to make sure that organic material tolerances and acidic medium tolerances are taken into account, because each of these factors is able to enhance the cycling durability under several conditions. In acidic conditions, it can be beneficial to utilize metallic catalysts with a lower active site such as Cu in order to protect the metal active sites, or it can be beneficial to develop metal-free catalytic systems comprising heteroatoms or metal active sites encapsulated in carbon to prevent them from being oxidized. In this study, we examined the relationship between MOF structure, composite composition, and electrochemical performance to profit from the understanding of the materials' perspective and their impact on the potential of particle-based components for the enhancement of high-performance Fuel-cell systems.

2.2. MOFs as Electrolyte Application

MOFs with high proton conductivities have recently attracted a lot of attention due to their outstanding properties. The coordination skeleton can deliver protons directly or through carrier particles [85,86]. MOFs, however, are restricted in their migration of proton conductors as a result of their grain-boundary structure, which leads to an insufficient conductivity. Furthermore, because of the unique and diverse crystal structures of MOFs, it is extremely hard to directly process them for direct use in fuel cells [87]. A practical solution to this problem is to combine MOFs with materials of a polymeric nature and their advancement as composite membranes [85,88].

It is generally possible to divide the PEMs modified by MOFs into two basic types. Phytic@MIL, PIL@MIL, and acids@MIL are some of the proton carriers that have been immersed in the pores of MOFs that can be used in this method. Moreover, an alternative approach is to augment the hydrophilic and acidic properties of MOFs by adding useful chemical components (-SO_3H, -NH_2, -2COOH) to the organic ligands [89–91]. Despite the excitement surrounding these findings, reports in this direction are scarce with much to discover about various MOFs. There will be a brief summary of the performance enhancements of PEMs by using different MOFs in this section, including the UIO-series, MIL-series, ZIF-series and other MOFs. A MOF has the advantage of being able to be customized to meet the specific requirements of any application. Because of their specific properties, MOFs might possess the ability to enhance nafion functionality, which is a state-of-the-art electrolyte, and thus improve water containment in structures and the proton conductivity of nafion-based layers. Polymers and MOF composites can normally be improved in their proton conductivity in two separate ways: either by saturating their pores with protons or by modifying their organic groups with functional moieties to provide them with increased hydrophobicity and acidity [92,93]. In this study, Yang et al. developed a high-performance composite membrane made from nafion and MOFs. They were interested in illustrating that graphene oxide (GO) can be grown on a porous metal-organic framework (ZIF-8) and subsequently be introduced into the nafion matrix. It was also found that ZIF-8 and GO had a synergetic effect that improved the proton conductivity by a significant amount [92].

In order to improve PEMFC performance, UIO-66 with high stability has been extensively studied. Recent research by Rao et al. revealed the use of nafion membranes for obtaining graphene nanosheets covalently bonded to UIO-66 (Figure 6a–c) [94].

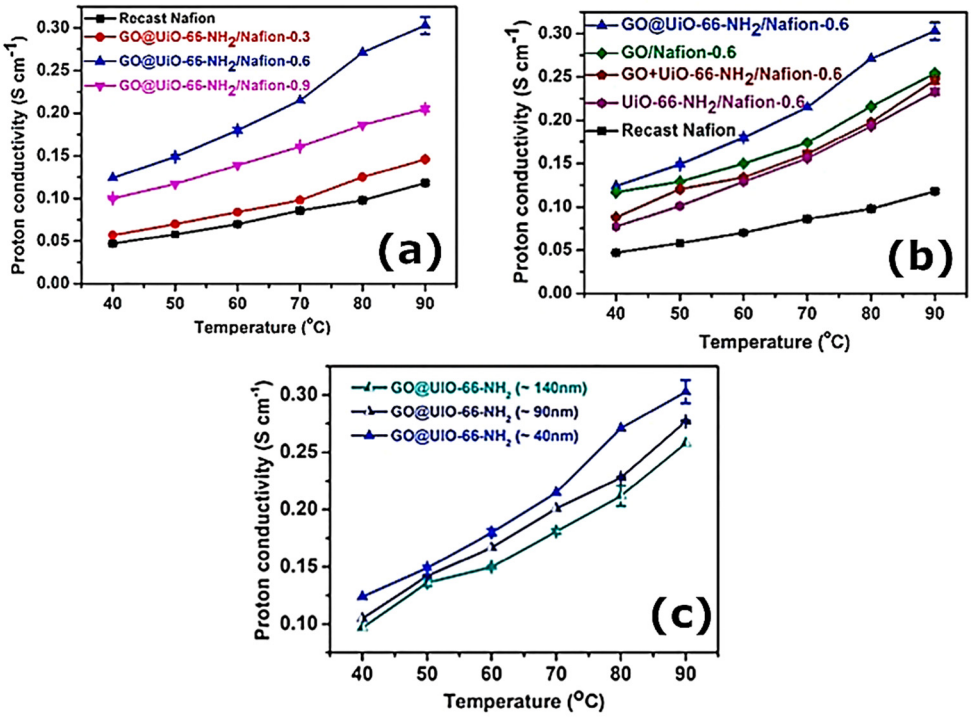

Figure 6. (**a**) Conductivity measurement plot of protons (at 95% RH) of nafion and nafion/NH_2-UiO-66@GO-fused membranes under variable loadings of NH_2-UiO-66@GO. (**b**) Proton conductivity measurements (at 95% RH) of nafion and different nafion membrane compositions with 0.6 wt.% filler content. (**c**) Proton conductivity measurements (at 95% RH) of nafion and nafion/NH_2-UiO-66@GO composite membranes with different NH2-UiO-66@GO sizes [94].

The aim of this study was to prepare different sizes of NH_2-UiO-66 for use in this experiment (40, 90, and 140 nm), which were then attached to polydopamine-coated GO. Interestingly, the conductivity varied with the filler content, which reached its maximum value when it was at 0.6 wt.%. In addition, it also depended on the MOF size, which was ideally 40 nm. MOFs have not been studied in detail for their mechanical properties or stability. In contrast to nafion membranes with smaller NH_2-UiO-66 (90 nm) and 140 nm, the proton permeability of nafion membranes with larger NH_2-UiO-66 (90 nm) was lower, most likely related to the large interconnection of NH_2-UiO-66 and the GO substrate, which may lead to an interruption in proton-transfer channels. As a result of UiO-66's remarkably high stability, the material has been extensively studied for potential applications in PEMFCs. Recently, an organic material designated porous organic cages has been shown to be a potential filler for proton-exchange membranes. The in situ crystallization of nafion matrixes with Cage 3 attached has been reported as shown in Figure 7a,b [95]. Cage 3 is known to possess intrinsic 3D channels that may assist proton conduction. A composite membrane can be greatly enhanced in terms of water-retention capacity by integrating Cage 3 into the nafion matrix, which is typically degraded at 320 °C (Figure 7c). Even though Cage 3 is potentially useful as a PEM, no mechanical studies have been conducted to determine the impact of incorporating it into a polymeric matrix. There was a significant improvement in proton conductivity when Cage 3 was added, but there was no substantial improvement in the methanol permeability. Under the same operating conditions, a nafion membrane containing Cage 3 achieved 0.27 S cm^{-1} with a mass fraction of 5% when heated to 90 °C and used at 95% relative humidity. This is a substantial improvement over recast nafion (0.08 S cm^{-1}) under identical conditions (Figure 7d,e).

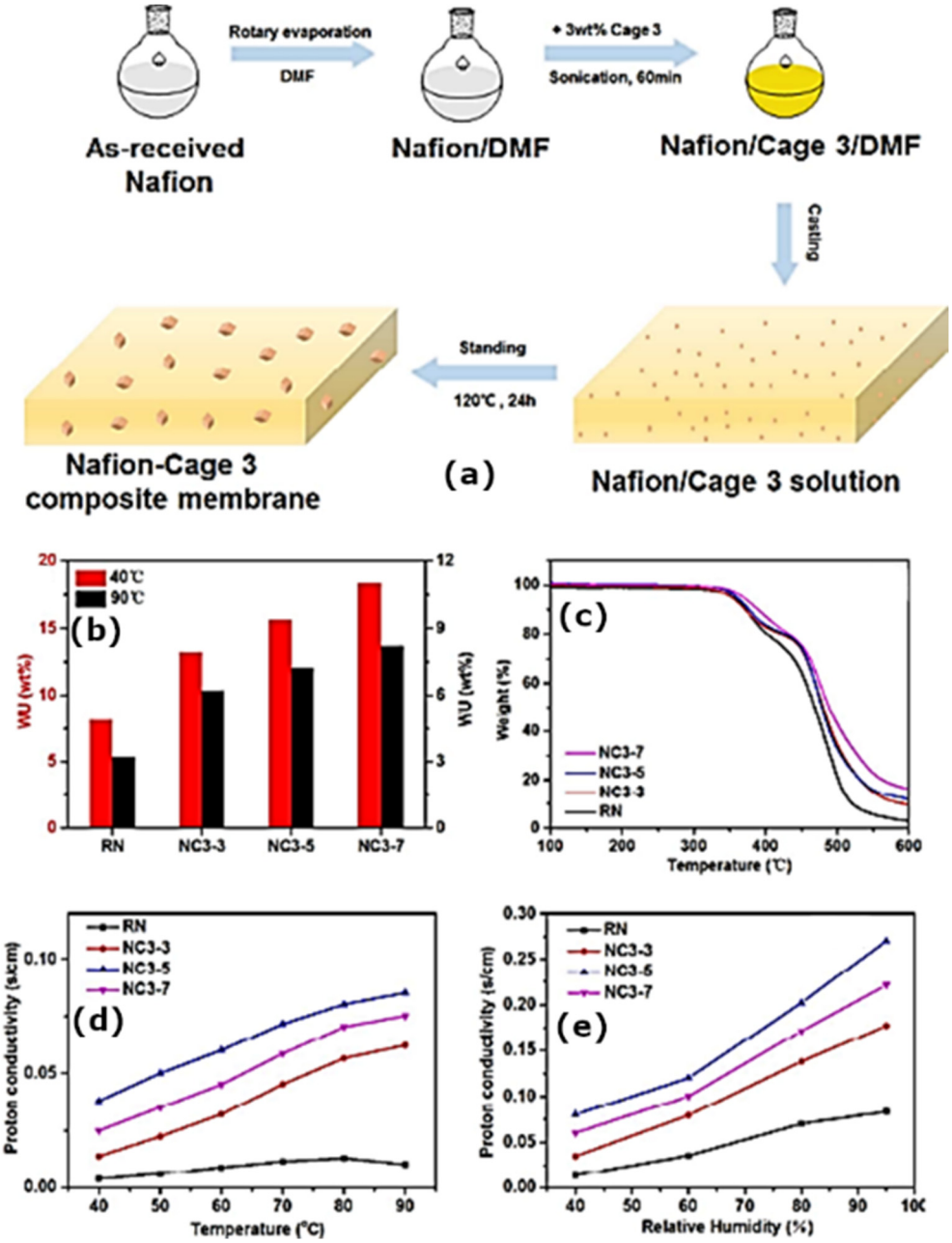

Figure 7. (**a**) Schematic illustration of preparation of nafion-Cage 3 composite membrane; (**b**,**c**) water-uptake capacity {WU (wt.%)} and thermogravimetric analysis (TGA) data of recast nafion and nafion-Cage 3 composite membrane; (**d**) dependence of temperature (40% RH); (**e**) dependence of humidity (90 °C) proton conductivity of recast nafion and nafion-Cage 3 composite membrane [95].

In addition, reports have been published about the use of non-classical MOFs, including nafion-based composites. Specifically, Wang et al. have identified MOF-W_1/nafion and MOF-W_2/nafion as two composite membranes, as shown in Figure 8 [96], which contain the same type of acid: 5,5′-(butane-1,4-diylbis(oxy)) di-isophthalic acid (H_4BDD). It appears that the molecular system MOF-W_1 has binuclear molecules that are connected through hydrogen atoms, primarily hydrogen bonds between uncoordinated carboxylic groups and water molecules. The MOF-W_2 is a supramolecular two-dimensional chain formed from one-dimensional hydrogen bonds between the uncoordinated and coordinated carboxylate groups. MOF-W_1/nafion and MOF-W_2/nafion have proton conductivity values of 4.04×10^{-7} and 4.94×10^{-7}, respectively, at 30 °C. Recently, Wang et al. studied the

impact of doping NH_3-modified Zn-MOF inside a nafion matrix. In order to improve the electrochemical performance of nafion hybrid membranes, NH_3-modified Zn-MOFs were embedded as guest molecules inside nafion as a host (Figure 9a) [97]. The proton conduction of the designed hybrid membranes was greatly enhanced by the diverse and abundant hydrogen bonds. Upon doping Zn-MOF in the nafion membrane, the conductivity enhancement was 1.87-fold purer than nafion, whereas by doping NH_3-Zn-MOF inside the nafion membrane, the conductivity enhancement was 5.47-times purer than nafion. In terms of performance, we see that 212-mW cm^{-2} of maximum power density and 660 mA cm^{-2} of maximum current density are both quite good for a single cell (Figure 9b). A comparison of proton conductivity of nafion/MOF-based hybrid electrolyte is shown in Table 2.

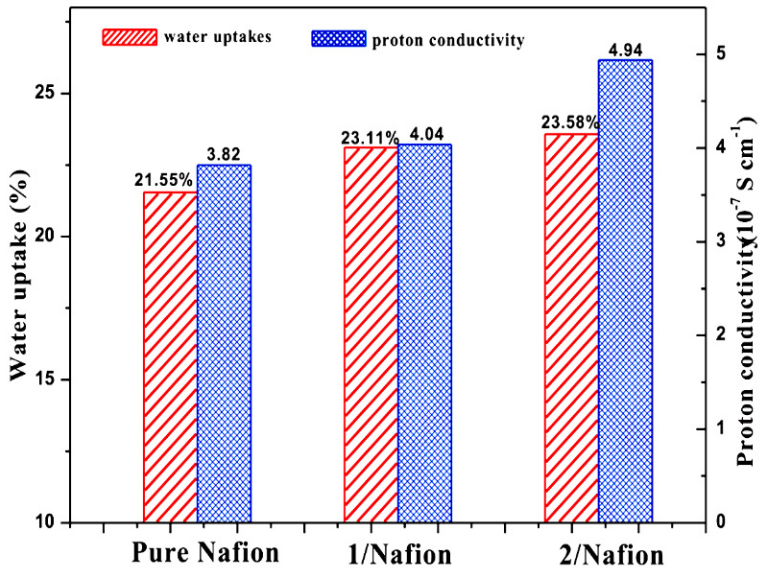

Figure 8. Proton conductivity and water uptake of nafion/W_1, nafion/W_2 and nafion membranes [96].

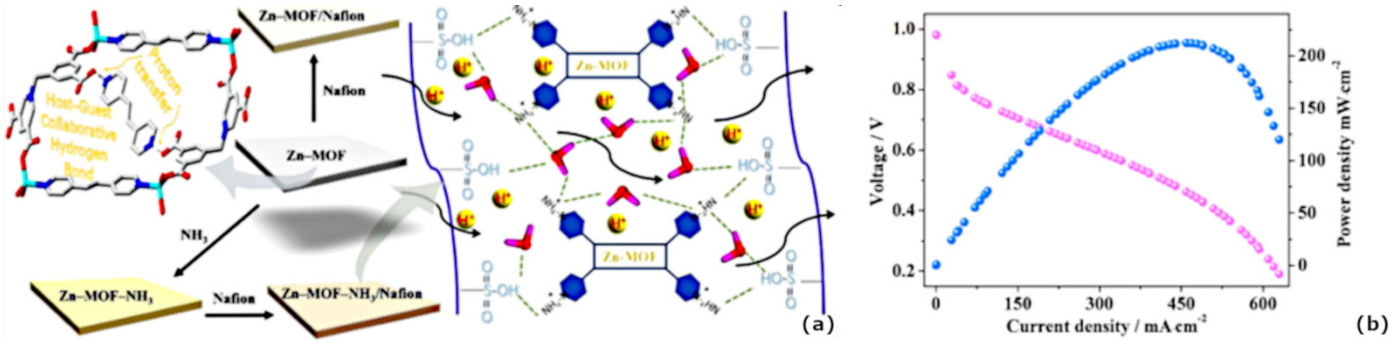

Figure 9. (**a**) Schematic diagram showing the synthesis of MOF engaging in host-guest associations specific to hydrogen bonding in the Zn-MOF structural unit, and (**b**) discrete H_2/O_2 Fuel-cell current-density-voltage plot of the hybrid membrane at 60 °C [97].

Table 2. Comparison of nafion/MOF-based hybrid electrolyte for Fuel-cell applications.

Filler	Polymer Backbone	Proton Conductivity (S cm^{-1})	Conditions
Cr-MIL-101-NH_2 [98]	SPES	4.1×10^{-2}	160 °C
UiO-66 [99]	Nafion	1.65×10^{-1}	80 °C, 95% RH
UiO-66-SO_3H [99]	Nafion	1.71×10^{-1}	80 °C, 95% RH
UiO-66-NH_2 [100]	Nafion	1.84×10^{-1}	80 °C, 95% RH
UiO-66-NH_2 + UiO-66-SO_3H [100]	Nafion	2.56×10^{-1}	90 °C, 95% RH
UiO-66-NH_2 + UiO-66-SO_3H [101]	Chitosan	5.2×10^{-2}	100 °C, 95% RH
GO@UiO-66-SO_3H [102]	SPEEK	2.68×10^{-1}	70 °C, 95% RH
GO@UiO-66-NH_2 [94]	Nafion	3.03×10^{-1}	90 °C, 95% RH
PWA@UiO-66-NH_2 [103]	Nafion	9.2×10^{-2}	Ambient condition
MIL-101 [104]	Chitosan	3.4×10^{-2}	100 °C, 100% RH
S-MIL-101 [104]	Chitosan	6.4×10^{-2}	100 °C, 100% RH
H_2SO_4@MIL-101 [104]	Chitosan	9.5×10^{-2}	100 °C, 100% RH
H_3PO_4@MIL-101 [104]	Chitosan	8.3×10^{-2}	100 °C, 100% RH
CF_3SO_3H@MIL-101 [104]	Chitosan	9.4×10^{-2}	100 °C, 100% RH
H_3P0_4/ZIF-8 [105]	PBI	3.1×10^{-3}	180 °C, anhydrous
H_3P0_4/ZIF-67 [105]	PBI	4.2×10^{-2}	180 °C, anhydrous
H_3P0_4/ZIF-mix [105]	PBI	9.2×10^{-2}	180 °C, anhydrous
ZIF-8 [106]	SPEEK	1.6×10^{-2}	100 °C
ZIF-67 [106]	SPEEK	1.5×10^{-2}	100 °C
ZIF-mix [106]	SPEEK	2.9×10^{-2}	100 °C
SO_3H-MIL-100(Fe) [107]	SPS	3.82×10^{-3}	25 °C, 100% RH
Polydopamine-ZIF-8 [108]	Nafion	2.5×10^{-1}	80 °C, 95% RH
polyacrylate carboxyl-ZIF-8 [109]	Nafion	2.4×10^{-1}	25 °C, 100% RH
Phytic@MIL101 [110]	Sulfonated poly (arylene ether ketone)	0.192	80 °C, 100% RH
MOF-1 [89]	Aquivion	3.49×10^{-2}	25 °C, 100% RH
Co-tri MOF [111]	Aquivion	5.06×10^{-2}	25 °C, 100% RH
SO_3H-MIL101 [112]	SPEEK	3.406×10^{-1}	75 °C, 100% RH
HPW-MIL-101(Cr) [113]	SPEEK	2.72×10^{-1}	65 °C, 100% RH
Cu–TMA [114]	SPEEK	4.5×10^{-2}	70 °C, 98% RH
MOF-801 [115]	C-SPAEKS	1.0×10^{-1}	90 °C, 100% RH
MIL-100(Fe) [116]	C-SPAEKS	1.38×10^{-1}	100 °C, 98% RH
Im@MOF-801 [117]	C-SPAEKS	1.28×10^{-1}	90 °C, 100% RH
MOF-5(SiO_2) [118]	SPEEK	3.69×10^{-3}	20 °C
MOF-Z1 [119]	SPEEK	3.95×10^{-3}	80 °C, 98% RH
MOF-Z2 [119]	SPEEK	3.17×10^{-3}	80 °C, 98% RH
ZIF-L [120]	SPEEK	1.83×10^{-1}	70 °C, 90% RH
SO_4-MOF-808 [121]	SPEEK	1.96×10^{-1}	70 °C, 90% RH
Fe-MIL-101-NH_2 [122]	SPPO	2.5×10^{-2}	90 °C, 98% RH
NAPI-Fe-MIL-101-NH_2 [123]	SPPO	4×10^{-2}	160 °C, 15% RH
Cd-MOF [124]	SPPO	2.64×10^{-2}	70 °C, 98% RH
MOF-azo [125]	Nafion	1.12×10^{-2}	Ambient conditions

Table 2. *Cont.*

Filler	Polymer Backbone	Proton Conductivity (S cm^{-1})	Conditions
MOF-bpy [125]	Nafion	2.6×10^{-2}	Ambient conditions
MOF-bpe [125]	Nafion	2.95×10^{-1}	Ambient conditions
ZIF-67 NFMs [126]	Nafion	2.88×10^{-1}	80 °C, 100% RH
ZHNFs [127]	Nafion	2.77×10^{-1}	80 °C, 100% RH
MOF-Mn1 [128]	Nafion	3.35×10^{-4}	70 °C, 30% RH
MOF-Mn2 [128]	Nafion	3.67×10^{-4}	70 °C, 30% RH
H_3PO_4/Ni-BDC [129]	PAN	1.05×10^{-2}	80 °C, 90% RH
Ni-BDC [129]	PAN	1.67×10^{-4}	80 °C, 90% RH
[BMIM]BF4@UiO-67) [130]	PAN	2.53×10^{-4}	90 °C, 35% RH
Ni-BDC [131]	PAN	6.04×10^{-5}	90 °C, 90% RH
Zr-Cr-SO_3H [132]	BSP	1.54×10^{-1}	80 °C, 100% RH
MOF-Z4 [133]	PVA	2.1×10^{-4}	65 °C, 98% RH
MOF-Z5 [133]	PVA	2.9×10^{-4}	65 °C, 98% RH
ZIF-8 [134]	PBI	3.1×10^{-3}	200 °C, anhydrous
ZIF-67 [134]	PBI	4.1×10^{-2}	200 °C, anhydrous
ZIF-8 + ZIF-67 [134]	PBI	9.1×10^{-2}	200 °C, anhydrous
MIL-100(Fe) [135]	sPSU	2.55×10^{-3}	25 °C, 100% RH
UiO-66-NH_2-Glu [136]	sPSU	2.1×10^{-1}	80 °C, 100% RH

SPES—sulfonated polyethersulfone; SPEEK—sulfonated poly(ether ether ketone); PBI—polybenzimidazole; SPS—sulfonated polysulfone; SPAEKs—sulfonated poly(arylene ether ketone)s; SPPO—sulfonated poly(phenylene oxide); PAN—polyacrylonitrile; BSP, PBA—poly(butyl acrylate); sPSU—sulfonated polysulfone; BSP—branched sulfonated polymer.

3. Conclusions and Perspective

Recent studies have demonstrated that MOFs hold a prominent position in electrochemistry due to their large surface area, excellent mass transfer, porosity and effective active sites. Inspired by this, we have systematically summarized various literature focussing on the use of MOFs in Fuel-cell systems in tabular form. At the present time, considerable efforts have been made to integrate MOF-based materials for commercial use. However, technical difficulties still exist for tuning the MOF chemistry towards Fuel-cell technologies for industrial production. By using environmentally friendly rechargeable batteries, we can reduce energy consumption and protect the environment. It is crucial to mention that fuel cells are proficient in directly converting chemical to electrical energy. This technology has become known for its ultra-high power density, excellent reaction efficiency, quick start-up, easy manufacturing, low operating temperatures, and convenience of industrial production. However, the electrochemical performance and the cost-effectiveness of these batteries need to be enhanced to ensure their long-term reliability and durability. To enable better enhance Fuel-cell-related performance technology at the present time, electrolytes and electrocatalysts need to be optimized for their interfacial effects. Further, proton-transport capacity has to be increased and the resistance must be reduced. Electrocatalytic reactions involving oxygen reduction reactions are substantially affected by the coordination surrounding the active sites inside MOFs. Real-time monitoring of degradation processes and electrocatalytic activity can improve Fuel-cell life and stability. There are still a variety of practical issues associated with Fuel-cell technology despite the major scientific and technological advancements in these fields. These issues may include local and material degradation and side reactions. In hindsight, one of the main factors restricting the commercial success of PEMFCs is their durability. Hence, the present scenario is to predict the process lifetime while making informed judgements about the degradation and performance of PEMFCs under Fuel-cell operation conditions.

Improvements in certainty will require more powerful and accurate practical models, and artificial-intelligence-based methods will be in demand [137–142].

Author Contributions: Conceptualization, A.K., V.K., P.P. and S.S.; investigation, A.K.; resources, A.K. and P.P.; data curation, A.K.; writing—original draft preparation, A.K.; writing—review and editing, A.K., V.K., S.S. and P.P.; visualization, A.K., V.K. and S.S.; supervision, V.K. and S.S.; project administration, V.K. and S.S.; funding acquisition V.K., S.S. and P.P. All authors have read and agreed to the published version of the manuscript.

Funding: This work acknowledges support from Basic Science Research Program through the National Research Foundation of Korea (NRF) funded by the Ministry of Science, ICT & Future Planning (No. 2022R1A2C1006090, 2017R1A2B4008801), NRF Basic Research Programme in Science and Engineering by the Ministry of Education (No. 2017R1D1A1B03036226). V.K. also thankfully acknowledges the support from the National Convergence Research of Scientific Challenges through the National Research Foundation of Korea (NRF) funded by Ministry of Science and ICT (No. 2021M3F7A1017476) and by the INDO-KOREA JNC program of the National Research Foundation of Korea Grant No. 2017K1A3A1A68.

Institutional Review Board Statement: Not Applicable.

Informed Consent Statement: Not applicable.

Conflicts of Interest: The authors declare no conflict of interest.

References

1. Meloni, E.; Iervolino, G.; Ruocco, C.; Renda, S.; Festa, G.; Martino, M.; Palma, V. Electrified Hydrogen Production from Methane for PEM Fuel Cells Feeding: A Review. *Energies* **2022**, *15*, 3588. [CrossRef]
2. Rossetti, I. Modelling of Fuel Cells and Related Energy Conversion Systems. *ChemEngineering* **2022**, *6*, 32. [CrossRef]
3. Alashkar, A.; Al-Othman, A.; Tawalbeh, M.; Qasim, M. A Critical Review on the Use of Ionic Liquids in Proton Exchange Membrane Fuel Cells. *Membranes* **2022**, *12*, 178. [CrossRef] [PubMed]
4. Kumar, A.; Hong, J.; Yun, Y.; Bhardwaj, A.; Song, S.-J. The Role of Surface Lattice Defects of CeO 2-δ Nanoparticles as a Scavenging Redox Catalyst in Polymer Electrolyte Membrane Fuel Cells. *J. Mater. Chem. A* **2020**, *8*, 26023–26034. [CrossRef]
5. Liu, Q.; Li, Z.; Wang, D.; Li, Z.; Peng, X.; Liu, C.; Zheng, P. Metal Organic Frameworks Modified Proton Exchange Membranes for Fuel Cells. *Front. Chem.* **2020**, *8*, 694. [CrossRef]
6. Anwar, R.; Iqbal, N.; Hanif, S.; Noor, T.; Shi, X.; Zaman, N.; Haider, D.; Rizvi, S.A.M.; Kannan, A.M. MOF-Derived CuPt/NC Electrocatalyst for Oxygen Reduction Reaction. *Catalysts* **2020**, *10*, 799. [CrossRef]
7. Delaporte, N.; Rivard, E.; Natarajan, S.K.; Benard, P.; Trudeau, M.L.; Zaghib, K. Synthesis and Performance of MOF-Based Non-Noble Metal Catalysts for the Oxygen Reduction Reaction in Proton-Exchange Membrane Fuel Cells: A Review. *Nanomaterials* **2020**, *10*, 1947. [CrossRef]
8. Wang, Y.; Liao, J.; Li, Z.; Wu, B.; Lou, J.; Zeng, L.; Zhao, T. Ir-Pt/C Composite with High Metal Loading as a High-Performance Anti-Reversal Anode Catalyst for Proton Exchange Membrane Fuel Cells. *Int. J. Hydrogen Energy* **2022**, *47*, 13101–13111. [CrossRef]
9. Tellez-Cruz, M.M.; Escorihuela, J.; Solorza-Feria, O.; Compañ, V. Proton Exchange Membrane Fuel Cells (PEMFCs): Advances and Challenges. *Polymers* **2021**, *13*, 3064. [CrossRef]
10. Yun, Y.; Kumar, A.; Hong, J.; Song, S.-J. Impact of CeO2 Nanoparticle Morphology: Radical Scavenging within the Polymer Electrolyte Membrane Fuel Cell. *J. Electrochem. Soc.* **2021**, *168*, 114521. [CrossRef]
11. Feng, L.; Wang, K.-Y.; Lv, X.-L.; Yan, T.-H.; Zhou, H.-C. Hierarchically Porous Metal-organic frameworks: Synthetic Strategies and Applications. *Natl. Sci. Rev.* **2019**, *7*, 1743–1758. [CrossRef] [PubMed]
12. Feng, L.; Yuan, S.; Zhang, L.-L.; Tan, K.; Li, J.-L.; Kirchon, A.; Liu, L.-M.; Zhang, P.; Han, Y.; Chabal, Y.J.; et al. Creating Hierarchical Pores by Controlled Linker Thermolysis in Multivariate Metal-organic frameworks. *J. Am. Chem. Soc.* **2018**, *140*, 2363–2372. [CrossRef] [PubMed]
13. Shen, K.; Zhang, L.; Chen, X.; Liu, L.; Zhang, D.; Han, Y.; Chen, J.; Long, J.; Luque, R.; Li, Y.; et al. Ordered Macro-Microporous Metal-Organic Framework Single Crystals. *Science* **2018**, *359*, 206–210. [CrossRef] [PubMed]
14. Feng, L.; Day, G.S.; Wang, K.-Y.; Yuan, S.; Zhou, H.-C. Strategies for Pore Engineering in Zirconium Metal-Organic Frameworks. *Chem* **2020**, *6*, 2902–2923. [CrossRef]
15. Lohse, M.S.; Bein, T. Covalent Organic Frameworks: Structures, Synthesis, and Applications. *Adv. Funct. Mater.* **2018**, *28*, 1705553. [CrossRef]
16. Baumann, A.E.; Burns, D.A.; Liu, B.; Thoi, V.S. Metal-Organic Framework Functionalization and Design Strategies for Advanced Electrochemical Energy Storage Devices. *Commun. Chem.* **2019**, *2*, 86. [CrossRef]
17. Zhao, R.; Xia, W.; Lin, C.; Sun, J.; Mahmood, A.; Wang, Q.; Qiu, B.; Tabassum, H.; Zou, R. A Pore-Expansion Strategy to Synthesize Hierarchically Porous Carbon Derived from Metal-Organic Framework for Enhanced Oxygen Reduction. *Carbon* **2017**, *114*, 284–290. [CrossRef]

18. Doan, H.V.; Amer Hamzah, H.; Karikkethu Prabhakaran, P.; Petrillo, C.; Ting, V.P. Hierarchical Metal-organic frameworks with Macroporosity: Synthesis, Achievements, and Challenges. *Nano-Micro Lett.* **2019**, *11*, 54. [CrossRef]
19. Feng, L.; Wang, K.-Y.; Willman, J.; Zhou, H.-C. Hierarchy in Metal-organic frameworks. *ACS Cent. Sci.* **2020**, *6*, 359–367. [CrossRef]
20. Zhao, Y.; Song, Z.; Li, X.; Sun, Q.; Cheng, N.; Lawes, S.; Sun, X. Metal Organic Frameworks for Energy Storage and Conversion. *Energy Storage Mater.* **2016**, *2*, 35–62. [CrossRef]
21. Furukawa, H.; Yaghi, O.M. Storage of Hydrogen, Methane, and Carbon Dioxide in Highly Porous Covalent Organic Frameworks for Clean Energy Applications. *J. Am. Chem. Soc.* **2009**, *131*, 8875–8883. [CrossRef] [PubMed]
22. Deng, H.; Grunder, S.; Cordova, K.E.; Valente, C.; Furukawa, H.; Hmadeh, M.; Gándara, F.; Whalley, A.C.; Liu, Z.; Asahina, S.; et al. Large-Pore Apertures in a Series of Metal-Organic Frameworks. *Science* **2012**, *336*, 1018–1023. [CrossRef] [PubMed]
23. Kumar, A.; Yun, Y.; Hong, J.; Kim, I.-H.; Bhardwaj, A.; Song, S.-J. Influence of Different Parameters on Total Fluoride Concentration Evaluation in Ex-Situ Chemical Degradation of Nafion Based Membrane. *Korean J. Chem. Eng.* **2021**, *38*, 2057–2063. [CrossRef]
24. Park, I.Y.; Hong, B.K.; Ko, J.J.; Kumar, A.; Song, S.J.; Hong, J. Antioxidant For Fuel Cells and Membrane-Electrode Assembly Including The Same. U.S. Patent 11,024,865, 1 June 2021.
25. Park, I.Y.; Oh, J.K.; Hong, B.K.; Kumar, A.; Song, S.J.; Hong, J.W. Membrane-Electrode Assembly for Fuel Cells with Improved Mechanical Strength and Proton Conductivity and Method of Manufacturing the Same. U.S. Patent 11,196,070, 7 December 2021.
26. Wang, H.; Yan, J.; Song, W.; Jiang, C.; Wang, Y.; Xu, T. Ion Exchange Membrane Related Processes towards Carbon Capture, Utilization and Storage: Current Trends and Perspectives. *Sep. Purif. Technol.* **2022**, *296*, 121390. [CrossRef]
27. Gagliardi, G.G.; Ibrahim, A.; Borello, D.; El-Kharouf, A. Composite Polymers Development and Application for Polymer Electrolyte Membrane Technologies—A Review. *Molecules* **2020**, *25*, 1712. [CrossRef]
28. Sulaiman, R.R.R.; Walvekar, R.; Wong, W.Y.; Khalid, M.; Pang, M.M. Proton Conductivity Enhancement at High Temperature on Polybenzimidazole Membrane Electrolyte with Acid-Functionalized Graphene Oxide Fillers. *Membranes* **2022**, *12*, 344. [CrossRef]
29. Ohkoshi, S.; Nakagawa, K.; Tomono, K.; Imoto, K.; Tsunobuchi, Y.; Tokoro, H. High Proton Conductivity in Prussian Blue Analogues and the Interference Effect by Magnetic Ordering. *J. Am. Chem. Soc.* **2010**, *132*, 6620–6621. [CrossRef]
30. Bureekaew, S.; Horike, S.; Higuchi, M.; Mizuno, M.; Kawamura, T.; Tanaka, D.; Yanai, N.; Kitagawa, S. One-Dimensional Imidazole Aggregate in Aluminium Porous Coordination Polymers with High Proton Conductivity. In *Materials For Sustainable Energy: A Collection of Peer-Reviewed Research and Review Articles from Nature Publishing Group*; World Scientific: Singapore, 2011; pp. 232–237.
31. Moi, R.; Ghorai, A.; Banerjee, S.; Biradha, K. Amino- and Sulfonate-Functionalized Metal–Organic Framework for Fabrication of Proton Exchange Membranes with Improved Proton Conductivity. *Cryst. Growth Des.* **2020**, *20*, 5557–5563. [CrossRef]
32. Pal, S.C.; Das, M.C. Superprotonic Conductivity of MOFs and Other Crystalline Platforms Beyond 10-1 S Cm-1. *Adv. Funct. Mater.* **2021**, *31*, 2101584. [CrossRef]
33. Wang, F.-D.; Wang, B.-C.; Hao, B.-B.; Zhang, C.-X.; Wang, Q.-L. Designable Guest-Molecule Encapsulation in Metal-organic frameworks for Proton Conductivity. *Chem. A Eur. J.* **2022**, *28*, e202103732. [CrossRef]
34. Lu, Z.; Wang, B.; Hu, Y.; Liu, W.; Zhao, Y.; Yang, R.; Li, Z.; Luo, J.; Chi, B.; Jiang, Z.; et al. An Isolated Zinc–Cobalt Atomic Pair for Highly Active and Durable Oxygen Reduction. *Angew. Chem. Int. Ed.* **2019**, *58*, 2622–2626. [CrossRef] [PubMed]
35. Wang, H.; Yin, F.-X.; Liu, N.; Kou, R.-H.; He, X.-B.; Sun, C.-J.; Chen, B.-H.; Liu, D.-J.; Yin, H.-Q. Engineering Fe–Fe3C@Fe–N–C Active Sites and Hybrid Structures from Dual Metal-organic frameworks for Oxygen Reduction Reaction in H_2–O_2 Fuel Cell and Li–O_2 Battery. *Adv. Funct. Mater.* **2019**, *29*, 1901531. [CrossRef]
36. Zhang, S.L.; Guan, B.Y.; Lou, X.W. Co–Fe Alloy/N-Doped Carbon Hollow Spheres Derived from Dual Metal-organic frameworks for Enhanced Electrocatalytic Oxygen Reduction. *Small* **2019**, *15*, 1805324. [CrossRef]
37. Guan, B.Y.; Lu, Y.; Wang, Y.; Wu, M.; Lou, X.W. Porous Iron–Cobalt Alloy/Nitrogen-Doped Carbon Cages Synthesized via Pyrolysis of Complex Metal–Organic Framework Hybrids for Oxygen Reduction. *Adv. Funct. Mater.* **2018**, *28*, 1706738. [CrossRef]
38. Yang, C.; Ma, X.; Zhou, J.; Zhao, Y.; Xiang, X.; Shang, H.; Zhang, B. Recent Advances in Metal-Organic Frameworks-Derived Carbon-Based Electrocatalysts for the Oxygen Reduction Reaction. *Int. J. Hydrogen Energy* **2022**, *47*, 21634–21661. [CrossRef]
39. Shahbazi Farahani, F.; Rahmanifar, M.S.; Noori, A.; El-Kady, M.F.; Hassani, N.; Neek-Amal, M.; Kaner, R.B.; Mousavi, M.F. Trilayer Metal-organic frameworks as Multifunctional Electrocatalysts for Energy Conversion and Storage Applications. *J. Am. Chem. Soc.* **2022**, *144*, 3411–3428. [CrossRef] [PubMed]
40. Cepitis, R.; Kongi, N.; Grozovski, V.; Ivaništšev, V.; Lust, E. Multifunctional Electrocatalysis on Single-Site Metal Catalysts: A Computational Perspective. *Catalysts* **2021**, *11*, 1165. [CrossRef]
41. Behera, P.; Subudhi, S.; Tripathy, S.P.; Parida, K. MOF Derived Nano-Materials: A Recent Progress in Strategic Fabrication, Characterization and Mechanistic Insight towards Divergent Photocatalytic Applications. *Coord. Chem. Rev.* **2022**, *456*, 214392. [CrossRef]
42. Song, Z.; Cheng, N.; Lushington, A.; Sun, X. Recent Progress on MOF-Derived Nanomaterials as Advanced Electrocatalysts in Fuel Cells. *Catalysts* **2016**, *6*, 116. [CrossRef]
43. Sun, Y.; Polani, S.; Luo, F.; Ott, S.; Strasser, P.; Dionigi, F. Advancements in Cathode Catalyst and Cathode Layer Design for Proton Exchange Membrane Fuel Cells. *Nat. Commun.* **2021**, *12*, 5984. [CrossRef]
44. Mølmen, L.; Eiler, K.; Fast, L.; Leisner, P.; Pellicer, E. Recent Advances in Catalyst Materials for Proton Exchange Membrane Fuel Cells. *APL Mater.* **2021**, *9*, 40702. [CrossRef]

45. Zhang, Q.; Guan, J. Applications of Atomically Dispersed Oxygen Reduction Catalysts in Fuel Cells and Zinc–Air Batteries. *Energy Environ. Mater.* **2021**, *4*, 307–335. [CrossRef]
46. Liu, X.; Li, Y.; Cao, Z.; Yin, Z.; Ma, T.; Chen, S. Current Progress of Metal Sulfides Derived from Metal-organic frameworks for Advanced Electrocatalysis: Potential Electrocatalysts with Diverse Applications. *J. Mater. Chem. A* **2022**, *10*, 1617–1641. [CrossRef]
47. Liu, H.; Yu, F.; Wu, K.; Xu, G.; Wu, C.; Liu, H.-K.; Dou, S.-X. Recent Progress on Fe-Based Single/Dual-Atom Catalysts for Zn–Air Batteries. *Small* **2022**, 2106635. [CrossRef]
48. Speck, F.D.; Kim, J.H.; Bae, G.; Joo, S.H.; Mayrhofer, K.J.J.; Choi, C.H.; Cherevko, S. Single-atom Catalysts: A Perspective toward Application in Electrochemical Energy Conversion. *JACS Au* **2021**, *1*, 1086–1100. [CrossRef]
49. Wang, Y.; Chu, F.; Zeng, J.; Wang, Q.; Naren, T.; Li, Y.; Cheng, Y.; Lei, Y.; Wu, F. Single Atom Catalysts for Fuel Cells and Rechargeable Batteries: Principles, Advances, and Opportunities. *ACS Nano* **2021**, *15*, 210–239. [CrossRef]
50. Zhang, Q.; Guan, J. Single-atom Catalysts for Electrocatalytic Applications. *Adv. Funct. Mater.* **2020**, *30*, 2000768. [CrossRef]
51. Song, Y.; Xie, W.; Shao, M.; Duan, X. Integrated Electrocatalysts Derived from Metal Organic Frameworks for Gas-Involved Reactions. *Nano Mater. Sci.* 2022, *in press*. [CrossRef]
52. Zhou, J.; Zeng, C.; Ou, H.; Yang, Q.; Xie, Q.; Zeb, A.; Lin, X.; Ali, Z.; Hu, L.; Zhou, J.; et al. Metal–Organic Framework-Based Materials for Full Cell Systems: A Review. *J. Mater. Chem. C* **2021**, *9*, 11030–11058. [CrossRef]
53. Yang, Y.; Fu, J.; Zhang, Y.; Ensafi, A.A.; Hu, J.-S. Molecular Engineering for Bottom-Up Construction of High-Performance Non-Precious-Metal Electrocatalysts with Well-Defined Active Sites. *J. Phys. Chem. C* **2021**, *125*, 22397–22420. [CrossRef]
54. Huang, H.; Shen, K.; Chen, F.; Li, Y. Metal-organic frameworks as a Good Platform for the Fabrication of Single-atom Catalysts. *ACS Catal.* **2020**, *10*, 6579–6586. [CrossRef]
55. Liu, Q.; Liu, X.; Zheng, L.; Shui, J. The Solid-Phase Synthesis of an Fe-N-C Electrocatalyst for High-Power Proton-Exchange Membrane Fuel Cells. *Angew. Chem. Int. Ed. Engl.* **2018**, *57*, 1204–1208. [CrossRef]
56. Chen, Y.; Ji, S.; Zhao, S.; Chen, W.; Dong, J.; Cheong, W.-C.; Shen, R.; Wen, X.; Zheng, L.; Rykov, A.I.; et al. Enhanced Oxygen Reduction with Single-atomic-Site Iron Catalysts for a Zinc-Air Battery and Hydrogen-Air Fuel Cell. *Nat. Commun.* **2018**, *9*, 5422. [CrossRef] [PubMed]
57. Deng, Y.; Chi, B.; Li, J.; Wang, G.; Zheng, L.; Shi, X.; Cui, Z.; Du, L.; Liao, S.; Zang, K.; et al. Atomic Fe-Doped MOF-Derived Carbon Polyhedrons with High Active-Center Density and Ultra-High Performance toward PEM Fuel Cells. *Adv. Energy Mater.* **2019**, *9*, 1802856. [CrossRef]
58. Deng, Y.; Chi, B.; Tian, X.; Cui, Z.; Liu, E.; Jia, Q.; Fan, W.; Wang, G.; Dang, D.; Li, M.; et al. G-C3N4 Promoted MOF Derived Hollow Carbon Nanopolyhedra Doped with High Density/Fraction of Single Fe Atoms as an Ultra-High Performance Non-Precious Catalyst towards Acidic ORR and PEM Fuel Cells. *J. Mater. Chem. A* **2019**, *7*, 5020–5030. [CrossRef]
59. Liu, S.; Meyer, Q.; Li, Y.; Zhao, T.; Su, Z.; Ching, K.; Zhao, C. Fe–N–C/Fe Nanoparticle Composite Catalysts for the Oxygen Reduction Reaction in Proton Exchange Membrane Fuel Cells. *Chem. Commun.* **2022**, *58*, 2323–2326. [CrossRef]
60. Qiao, M.; Wang, Y.; Wang, Q.; Hu, G.; Mamat, X.; Zhang, S.; Wang, S. Hierarchically Ordered Porous Carbon with Atomically Dispersed FeN4 for Ultraefficient Oxygen Reduction Reaction in Proton-Exchange Membrane Fuel Cells. *Angew. Chem. Int. Ed.* **2020**, *59*, 2688–2694. [CrossRef]
61. Li, J.; Chen, M.; Cullen, D.A.; Hwang, S.; Wang, M.; Li, B.; Liu, K.; Karakalos, S.; Lucero, M.; Zhang, H.; et al. Atomically Dispersed Manganese Catalysts for Oxygen Reduction in Proton-Exchange Membrane Fuel Cells. *Nat. Catal.* **2018**, *1*, 935–945. [CrossRef]
62. Wang, X.X.; Cullen, D.A.; Pan, Y.-T.; Hwang, S.; Wang, M.; Feng, Z.; Wang, J.; Engelhard, M.H.; Zhang, H.; He, Y.; et al. Nitrogen-Coordinated Single Cobalt Atom Catalysts for Oxygen Reduction in Proton Exchange Membrane Fuel Cells. *Adv. Mater.* **2018**, *30*, 1706758. [CrossRef]
63. Deng, Y.; Tian, X.; Chi, B.; Wang, Q.; Ni, W.; Gao, Y.; Liu, Z.; Luo, J.; Lin, C.; Ling, L.; et al. Hierarchically Open-Porous Carbon Networks Enriched with Exclusive Fe–Nx Active Sites as Efficient Oxygen Reduction Catalysts towards Acidic H2–O2 PEM Fuel Cell and Alkaline Zn–Air Battery. *Chem. Eng. J.* **2020**, *390*, 124479. [CrossRef]
64. He, Y.; Hwang, S.; Cullen, D.A.; Uddin, M.A.; Langhorst, L.; Li, B.; Karakalos, S.; Kropf, A.J.; Wegener, E.C.; Sokolowski, J.; et al. Highly Active Atomically Dispersed CoN4 Fuel Cell Cathode Catalysts Derived from Surfactant-Assisted MOFs: Carbon-Shell Confinement Strategy. *Energy Environ. Sci.* **2019**, *12*, 250–260. [CrossRef]
65. Zhang, L.; Li, L.; Gao, Z.; Guo, L.; Li, M.; Su, J. Porous Hierarchical Iron/Nitrogen Co-Doped Carbon Etched by g-C3N4 Pyrolysis as Efficient Non-Noble Metal Catalysts for PEM Fuel Cells. *ChemElectroChem* **2022**, *9*, e202101681. [CrossRef]
66. Yang, H.; Chen, X.; Chen, W.-T.; Wang, Q.; Cuello, N.C.; Nafady, A.; Al-Enizi, A.M.; Waterhouse, G.I.N.; Goenaga, G.A.; Zawodzinski, T.A.; et al. Tunable Synthesis of Hollow Metal-Nitrogen-Carbon Capsules for Efficient Oxygen Reduction Catalysis in Proton Exchange Membrane Fuel Cells. *ACS Nano* **2019**, *13*, 8087–8098. [CrossRef]
67. Zhou, Y.; Yang, W.; Utetiwabo, W.; Lian, Y.; Yin, X.; Zhou, L.; Yu, P.; Chen, R.; Sun, S. Revealing of Active Sites and Catalytic Mechanism in N-Coordinated Fe, Ni Dual-Doped Carbon with Superior Acidic Oxygen Reduction than Single-atom Catalyst. *J. Phys. Chem. Lett.* **2020**, *11*, 1404–1410. [CrossRef]
68. Zhong, H.; Wang, J.; Zhang, Y.; Xu, W.; Xing, W.; Xu, D.; Zhang, Y.; Zhang, X. ZIF-8 Derived Graphene-Based Nitrogen-Doped Porous Carbon Sheets as Highly Efficient and Durable Oxygen Reduction Electrocatalysts. *Angew. Chem. Int. Ed. Engl.* **2014**, *53*, 14235–14239. [CrossRef] [PubMed]

69. Jahan, M.; Liu, Z.; Loh, K.P. A Graphene Oxide and Copper-Centered Metal Organic Framework Composite as a Tri-Functional Catalyst for HER, OER, and ORR. *Adv. Funct. Mater.* **2013**, *23*, 5363–5372. [CrossRef]
70. Zhan, Y.; Xie, F.; Zhang, H.; Jin, Y.; Meng, H.; Chen, J.; Sun, X. Highly Dispersed Nonprecious Metal Catalyst for Oxygen Reduction Reaction in Proton Exchange Membrane Fuel Cells. *ACS Appl. Mater. Interfaces* **2020**, *12*, 17481–17491. [CrossRef] [PubMed]
71. Xu, M.; Chen, H.; Zhao, Y.; Ni, W.; Liu, M.; Xue, Y.; Huo, S.; Wu, L.; Yang, Z.; Yan, Y.-M. Ultrathin-Carbon-Layer-Protected PtCu Nanoparticles Encapsulated in Carbon Capsules: A Structure Engineering of the Anode Electrocatalyst for Direct Formic Acid Fuel Cells. *Part. Part. Syst. Charact.* **2019**, *36*, 1900100. [CrossRef]
72. Zhang, L.; Hu, Y.; Chen, J.; Huang, W.; Cheng, J.; Chen, Y. A Novel Metal Organic Framework-Derived Carbon-Based Catalyst for Oxygen Reduction Reaction in a Microbial Fuel Cell. *J. Power Sources* **2018**, *384*, 98–106. [CrossRef]
73. Macchi, S.; Denmark, I.; Le, T.; Forson, M.; Bashiru, M.; Jalihal, A.; Siraj, N. Recent Advancements in the Synthesis and Application of Carbon-Based Catalysts in the ORR. *Electrochem* **2021**, *3*, 1–27. [CrossRef]
74. Wang, X.; Li, Z.; Qu, Y.; Yuan, T.; Wang, W.; Wu, Y.; Li, Y. Review of Metal Catalysts for Oxygen Reduction Reaction: From Nanoscale Engineering to Atomic Design. *Chem* **2019**, *5*, 1486–1511. [CrossRef]
75. Kuzmin, A.V.; Shainyan, B.A. Theoretical Density Functional Theory Study of Electrocatalytic Activity of MN4-Doped (M = Cu, Ag, and Zn) Single-Walled Carbon Nanotubes in Oxygen Reduction Reactions. *ACS Omega* **2021**, *6*, 374–387. [CrossRef] [PubMed]
76. Liu, J.; Ma, J.; Zhang, Z.; Qin, Y.; Wang, Y.-J.; Wang, Y.; Tan, R.; Duan, X.; Tian, T.Z.; Zhang, C.H.; et al. 2021 Roadmap: Electrocatalysts for Green Catalytic Processes. *J. Phys. Mater.* **2021**, *4*, 22004. [CrossRef]
77. Zhang, H.; Ding, S.; Hwang, S.; Zhao, X.; Su, D.; Xu, H.; Yang, H.; Wu, G. Atomically Dispersed Iron Cathode Catalysts Derived from Binary Ligand-Based Zeolitic Imidazolate Frameworks with Enhanced Stability for PEM Fuel Cells. *J. Electrochem. Soc.* **2019**, *166*, F3116–F3122. [CrossRef]
78. Tang, C.; Chen, L.; Li, H.; Li, L.; Jiao, Y.; Zheng, Y.; Xu, H.; Davey, K.; Qiao, S.-Z. Tailoring Acidic Oxygen Reduction Selectivity on Single-atom Catalysts via Modification of First and Second Coordination Spheres. *J. Am. Chem. Soc.* **2021**, *143*, 7819–7827. [CrossRef]
79. Shen, S.; Sun, Y.; Sun, H.; Pang, Y.; Xia, S.; Chen, T.; Zheng, S.; Yuan, T. Research Progress in ZIF-8 Derived Single Atomic Catalysts for Oxygen Reduction Reaction. *Catalysts* **2022**, *12*, 525. [CrossRef]
80. Wang, J.; Huang, Z.; Liu, W.; Chang, C.; Tang, H.; Li, Z.; Chen, W.; Jia, C.; Yao, T.; Wei, S.; et al. Design of N-Coordinated Dual-Metal Sites: A Stable and Active Pt-Free Catalyst for Acidic Oxygen Reduction Reaction. *J. Am. Chem. Soc.* **2017**, *139*, 17281–17284. [CrossRef] [PubMed]
81. Miao, Z.; Wang, X.; Tsai, M.-C.; Jin, Q.; Liang, J.; Ma, F.; Wang, T.; Zheng, S.; Hwang, B.-J.; Huang, Y.; et al. Atomically Dispersed Fe-Nx/C Electrocatalyst Boosts Oxygen Catalysis via a New Metal-Organic Polymer Supramolecule Strategy. *Adv. Energy Mater.* **2018**, *8*, 1801226. [CrossRef]
82. He, Y.; Wu, G. PGM-Free Oxygen-Reduction Catalyst Development for Proton-Exchange Membrane Fuel Cells: Challenges, Solutions, and Promises. *Accounts Mater. Res.* **2022**, *3*, 224–236. [CrossRef]
83. Wei, Y.-S.; Zou, L.; Wang, H.-F.; Wang, Y.; Xu, Q. Micro/Nano-Scaled Metal-Organic Frameworks and Their Derivatives for Energy Applications. *Adv. Energy Mater.* **2022**, *12*, 2003970. [CrossRef]
84. Zhang, X.; Zhang, S.; Tang, Y.; Huang, X.; Pang, H. Recent Advances and Challenges of Metal–Organic Framework/Graphene-Based Composites. *Compos. Part B Eng.* **2022**, *230*, 109532. [CrossRef]
85. Nik Zaiman, N.F.H.; Shaari, N.; Harun, N.A.M. Developing Metal-Organic Framework-Based Composite for Innovative Fuel Cell Application: An Overview. *Int. J. Energy Res.* **2022**, *46*, 471–504. [CrossRef]
86. Yang, Z.; Zhang, N.; Lei, L.; Yu, C.; Ding, J.; Li, P.; Chen, J.; Li, M.; Ling, S.; Zhuang, X.; et al. Supramolecular Proton Conductors Self-assembled by Organic Cages. *JACS Au* **2022**, *2*, 819–826. [CrossRef] [PubMed]
87. Chen, L.; Wang, H.F.; Li, C.; Xu, Q. Bimetallic Metal-Organic Frameworks and Their Derivatives. *Chem. Sci.* **2020**, *11*, 5369–5403. [CrossRef]
88. Sajid, A.; Pervaiz, E.; Ali, H.; Noor, T.; Baig, M.M. A Perspective on Development of Fuel Cell Materials: Electrodes and Electrolyte. *Int. J. Energy Res.* **2022**, *46*, 6953–6988. [CrossRef]
89. Paul, S.; Choi, S.-J.; Kim, H.J. Enhanced Proton Conductivity of a Zn(II)-Based MOF/Aquivion Composite Membrane for PEMFC Applications. *Energy Fuels* **2020**, *34*, 10067–10077. [CrossRef]
90. Harun, N.A.M.; Shaari, N.; Nik Zaiman, N.F.H. A Review of Alternative Polymer Electrolyte Membrane for Fuel Cell Application Based on Sulfonated Poly(Ether Ether Ketone). *Int. J. Energy Res.* **2021**, *45*, 19671–19708. [CrossRef]
91. Ye, Y.; Gong, L.; Xiang, S.; Zhang, Z.; Chen, B. Metal-organic frameworks as a Versatile Platform for Proton Conductors. *Adv. Mater.* **2020**, *32*, 1907090. [CrossRef]
92. Yang, L.; Tang, B.; Wu, P. Metal–Organic Framework–Graphene Oxide Composites: A Facile Method to Highly Improve the Proton Conductivity of PEMs Operated under Low Humidity. *J. Mater. Chem. A* **2015**, *3*, 15838–15842. [CrossRef]
93. Nguyen, M.V.; Lo, T.H.N.; Luu, L.C.; Nguyen, H.T.T.; Tu, T.N. Enhancing Proton Conductivity in a Metal–Organic Framework at T > 80 °C by an Anchoring Strategy. *J. Mater. Chem. A* **2018**, *6*, 1816–1821. [CrossRef]
94. Rao, Z.; Feng, K.; Tang, B.; Wu, P. Construction of Well Interconnected Metal-Organic Framework Structure for Effectively Promoting Proton Conductivity of Proton Exchange Membrane. *J. Memb. Sci.* **2017**, *533*, 160–170. [CrossRef]

95. Han, R.; Wu, P. Composite Proton-Exchange Membrane with Highly Improved Proton Conductivity Prepared by in Situ Crystallization of Porous Organic Cage. *ACS Appl. Mater. Interfaces* **2018**, *10*, 18351–18358. [CrossRef] [PubMed]
96. Li, R.-Y.; Liu, H.-T.; Chu, Z.-T.; Zhou, C.-C.; Lu, J.; Wang, S.-N. Two Nonporous MOFs with Uncoordinated Carboxylate Groups: Fillers for Enhancing the Proton Conductivities of Nafion Membrane. *J. Solid State Chem.* **2020**, *281*, 121020. [CrossRef]
97. Wang, H.; Zhao, Y.; Shao, Z.; Xu, W.; Wu, Q.; Ding, X.; Hou, H. Proton Conduction of Nafion Hybrid Membranes Promoted by NH3-Modified Zn-MOF with Host–Guest Collaborative Hydrogen Bonds for H_2/O_2 Fuel Cell Applications. *ACS Appl. Mater. Interfaces* **2021**, *13*, 7485–7497. [CrossRef] [PubMed]
98. Anahidzade, N.; Abdolmaleki, A.; Dinari, M.; Firouz Tadavani, K.; Zhiani, M. Metal-Organic Framework Anchored Sulfonated Poly(Ether Sulfone) as a High Temperature Proton Exchange Membrane for Fuel Cells. *J. Memb. Sci.* **2018**, *565*, 281–292. [CrossRef]
99. Donnadio, A.; Narducci, R.; Casciola, M.; Marmottini, F.; D'Amato, R.; Jazestani, M.; Chiniforoshan, H.; Costantino, F. Mixed Membrane Matrices Based on Nafion/UiO-66/SO3H-UiO-66 Nano-MOFs: Revealing the Effect of Crystal Size, Sulfonation, and Filler Loading on the Mechanical and Conductivity Properties. *ACS Appl. Mater. Interfaces* **2017**, *9*, 42239–42246. [CrossRef]
100. Rao, Z.; Tang, B.; Wu, P. Proton Conductivity of Proton Exchange Membrane Synergistically Promoted by Different Functionalized Metal-organic frameworks. *ACS Appl. Mater. Interfaces* **2017**, *9*, 22597–22603. [CrossRef]
101. Dong, X.-Y.; Wang, J.-H.; Liu, S.-S.; Han, Z.; Tang, Q.-J.; Li, F.-F.; Zang, S.-Q. Synergy between Isomorphous Acid and Basic Metal-organic frameworks for Anhydrous Proton Conduction of Low-Cost Hybrid Membranes at High Temperatures. *ACS Appl. Mater. Interfaces* **2018**, *10*, 38209–38216. [CrossRef]
102. Sun, H.; Tang, B.; Wu, P. Rational Design of S-UiO-66@GO Hybrid Nanosheets for Proton Exchange Membranes with Significantly Enhanced Transport Performance. *ACS Appl. Mater. Interfaces* **2017**, *9*, 26077–26087. [CrossRef]
103. Yang, X.-B.; Zhao, L.; Goh, K.; Sui, X.; Meng, L.-H.; Wang, Z.-B. Ultra-High Ion Selectivity of a Modified Nafion Composite Membrane for Vanadium Redox Flow Battery by Incorporation of Phosphotungstic Acid Coupled UiO-66-NH2. *ChemistrySelect* **2019**, *4*, 4633–4641. [CrossRef]
104. Dong, X.-Y.; Li, J.-J.; Han, Z.; Duan, P.-G.; Li, L.-K.; Zang, S.-Q. Tuning the Functional Substituent Group and Guest of Metal-organic frameworks in Hybrid Membranes for Improved Interface Compatibility and Proton Conduction. *J. Mater. Chem. A* **2017**, *5*, 3464–3474. [CrossRef]
105. Escorihuela, J.; Sahuquillo, Ó.; García-Bernabé, A.; Giménez, E.; Compañ, V. Phosphoric Acid Doped Polybenzimidazole (PBI)/Zeolitic Imidazolate Framework Composite Membranes with Significantly Enhanced Proton Conductivity under Low Humidity Conditions. *Nanomaterials* **2018**, *8*, 775. [CrossRef] [PubMed]
106. Barjola, A.; Escorihuela, J.; Andrio, A.; Giménez, E.; Compañ, V. Enhanced Conductivity of Composite Membranes Based on Sulfonated Poly(Ether Ether Ketone) (SPEEK) with Zeolitic Imidazolate Frameworks (ZIFs). *Nanomaterials* **2018**, *8*, 1042. [CrossRef] [PubMed]
107. Roshanravan, B.; Younesi, H.; Abdollahi, M.; Rahimnejad, M.; Pyo, S.-H. Incorporating Sulfonated MIL-100(Fe) in Sulfonated Polysulfone for Enhancing Microbial Fuel Cell Performance. *Fuel* **2022**, *312*, 122962. [CrossRef]
108. Rao, Z.; Lan, M.; Wang, Z.; Wan, H.; Li, G.; Zhu, J.; Tang, B.; Liu, H. Effectively Facilitating the Proton Conduction of Proton Exchange Membrane by Polydopamine Modified Hollow Metal-organic Framework. *J. Memb. Sci.* **2022**, *644*, 120098. [CrossRef]
109. Zhu, L.; Li, Y.; Zhao, J.; Liu, J.; Wang, L.; Lei, J.; Xue, R. Enhanced Proton Conductivity of Nafion Membrane Induced by Incorporation of MOF-Anchored 3D Microspheres: A Superior and Promising Membrane for Fuel Cell Applications. *Chem. Commun.* **2022**, *58*, 2906–2909. [CrossRef]
110. Ru, C.; Li, Z.; Zhao, C.; Duan, Y.; Zhuang, Z.; Bu, F.; Na, H. Enhanced Proton Conductivity of Sulfonated Hybrid Poly(Arylene Ether Ketone) Membranes by Incorporating an Amino–Sulfo Bifunctionalized Metal–Organic Framework for Direct Methanol Fuel Cells. *ACS Appl. Mater. Interfaces* **2018**, *10*, 7963–7973. [CrossRef]
111. Paul, S.; Choi, S.-J.; Kim, H.J. Co-Tri MOF-Impregnated Aquivion® Composites as Proton Exchange Membranes for Fuel Cell Applications. *Ionics* **2021**, *27*, 1653–1666. [CrossRef]
112. Li, Z.; He, G.; Zhao, Y.; Cao, Y.; Wu, H.; Li, Y.; Jiang, Z. Enhanced Proton Conductivity of Proton Exchange Membranes by Incorporating Sulfonated Metal-Organic Frameworks. *J. Power Sources* **2014**, *262*, 372–379. [CrossRef]
113. Zhang, B.; Cao, Y.; Li, Z.; Wu, H.; Yin, Y.; Cao, L.; He, X.; Jiang, Z. Proton Exchange Nanohybrid Membranes with High Phosphotungstic Acid Loading within Metal-Organic Frameworks for PEMFC Applications. *Electrochim. Acta* **2017**, *240*, 186–194. [CrossRef]
114. Niluroutu, N.; Pichaimuthu, K.; Sarmah, S.; Dhanasekaran, P.; Shukla, A.; Unni, S.M.; Bhat, S.D. A Copper–Trimesic Acid Metal–Organic Framework Incorporated Sulfonated Poly(Ether Ether Ketone) Based Polymer Electrolyte Membrane for Direct Methanol Fuel Cells. *New J. Chem.* **2018**, *42*, 16758–16765. [CrossRef]
115. Ren, J.; Xu, J.; Ju, M.; Chen, X.; Zhao, P.; Meng, L.; Lei, J.; Wang, Z. Long-Term Durable Anion Exchange Membranes Based on Imidazole-Functionalized Poly(Ether Ether Ketone) Incorporating Cationic Metal-organic Framework. *Adv. Powder Mater.* **2022**, *1*, 100017. [CrossRef]
116. Zhang, Z.; Ren, J.; Xu, J.; Meng, L.; Zhao, P.; Wang, H.; Wang, Z. Enhanced Proton Conductivity of Sulfonated Poly(Arylene Ether Ketone Sulfone) Polymers by Incorporating Phosphotungstic Acid-Ionic-Liquid-Functionalized Metal-Organic Framework. *J. Memb. Sci.* **2021**, *630*, 119304. [CrossRef]

117. Zhang, Z.; Ren, J.; Xu, J.; Wang, Z.; He, W.; Wang, S.; Yang, X.; Du, X.; Meng, L.; Zhao, P. Adjust the Arrangement of Imidazole on the Metal-Organic Framework to Obtain Hybrid Proton Exchange Membrane with Long-Term Stable High Proton Conductivity. *J. Memb. Sci.* **2020**, *607*, 118194. [CrossRef]
118. Bisht, S.; Balaguru, S.; Ramachandran, S.K.; Gangasalam, A.; Kweon, J. Proton Exchange Composite Membranes Comprising SiO2, Sulfonated SiO2, and Metal-organic frameworks Loaded in SPEEK Polymer for Fuel Cell Applications. *J. Appl. Polym. Sci.* **2021**, *138*, 50530. [CrossRef]
119. Liu, X.-T.; Wang, B.-C.; Hao, B.-B.; Zhang, C.-X.; Wang, Q.-L. Dual-Functional Coordination Polymers with High Proton Conduction Behaviour and Good Luminescence Properties. *Dalt. Trans.* **2021**, *50*, 8718–8726. [CrossRef]
120. Cai, Y.Y.; Zhang, Q.G.; Zhu, A.M.; Liu, Q.L. Two-Dimensional Metal-Organic Framework-Graphene Oxide Hybrid Nanocomposite Proton Exchange Membranes with Enhanced Proton Conduction. *J. Colloid Interface Sci.* **2021**, *594*, 593–603. [CrossRef]
121. Cai, Y.Y.; Wang, J.J.; Cai, Z.H.; Zhang, Q.G.; Zhu, A.M.; Liu, Q.L. Enhanced Performance of Sulfonated Poly(Ether Ether Ketone) Hybrid Membranes by Introducing Sulfated MOF-808/Graphene Oxide Composites. *ACS Appl. Energy Mater.* **2021**, *4*, 9664–9672. [CrossRef]
122. Wu, B.; Lin, X.; Ge, L.; Wu, L.; Xu, T. A Novel Route for Preparing Highly Proton Conductive Membrane Materials with Metal-Organic Frameworks. *Chem. Commun.* **2013**, *49*, 143–145. [CrossRef]
123. Wu, B.; Liang, G.; Lin, X.; Wu, L.; Luo, J.; Xu, T. Immobilization of N-(3-Aminopropyl)-Imidazole through MOFs in Proton Conductive Membrane for Elevated Temperature Anhydrous Applications. *J. Memb. Sci.* **2014**, *458*, 86–95. [CrossRef]
124. Wang, F.-D.; Su, W.-H.; Zhang, C.-X.; Wang, Q.-L. High Proton Conductivity of a Cadmium Metal-Organic Framework Constructed from Pyrazolecarboxylate and Its Hybrid Membrane. *Inorg. Chem.* **2021**, *60*, 16337–16345. [CrossRef] [PubMed]
125. Wang, H.; Wen, T.; Shao, Z.; Zhao, Y.; Cui, Y.; Gao, K.; Xu, W.; Hou, H. High Proton Conductivity in Nafion/Ni-MOF Composite Membranes Promoted by Ligand Exchange under Ambient Conditions. *Inorg. Chem.* **2021**, *60*, 10492–10501. [CrossRef] [PubMed]
126. Zhao, G.; Shi, L.; Zhang, M.; Cheng, B.; Yang, G.; Zhuang, X. Self-Assembly of Metal-Organic Framework onto Nanofibrous Mats to Enhance Proton Conductivity for Proton Exchange Membrane. *Int. J. Hydrogen Energy* **2021**, *46*, 36415–36423. [CrossRef]
127. Ju, J.; Shi, J.; Wang, M.; Wang, L.; Cheng, B.; Yu, X.; Cai, Y.; Wang, S.; Fang, L.; Kang, W. Constructing Interconnected Nanofibers@ZIF-67 Superstructure in Nafion Membranes for Accelerating Proton Transport and Confining Methanol Permeation. *Int. J. Hydrogen Energy* **2021**, *46*, 38782–38794. [CrossRef]
128. Zhu, J.; Zhu, P.; Mei, J.; Xie, J.; Guan, J.; Zhang, K.-L. Proton Conduction and Luminescent Sensing Property of Two Newly Constructed Positional Isomer-Dependent Redox-Active Mn(II)-Organic Frameworks. *Polyhedron* **2021**, *200*, 115139. [CrossRef]
129. Bai, Z.; Liu, S.; Cheng, G.; Wu, G.; Liu, Y. High Proton Conductivity of MOFs-Polymer Composite Membranes by Phosphoric Acid Impregnation. *Microporous Mesoporous Mater.* **2020**, *292*, 109763. [CrossRef]
130. Chen, P.; Liu, S.; Bai, Z.; Liu, Y. Enhanced Ionic Conductivity of Ionic Liquid Confined in UiO-67 Membrane at Low Humidity. *Microporous Mesoporous Mater.* **2020**, *305*, 110369. [CrossRef]
131. Bai, Z.; Liu, S.; Chen, P.; Cheng, G.; Wu, G.; Liu, Y. Enhanced Proton Conduction of Imidazole Localized in One-Dimensional Ni-Metal-Organic Framework Nanofibers. *Nanotechnology* **2020**, *31*, 125702. [CrossRef]
132. Neelakandan, S.; Ramachandran, R.; Fang, M.; Wang, L. Improving the Performance of Sulfonated Polymer Membrane by Using Sulfonic Acid Functionalized Hetero-Metallic Metal-Organic Framework for DMFC Applications. *Int. J. Energy Res.* **2020**, *44*, 1673–1684. [CrossRef]
133. Yang, S.-L.; Sun, P.-P.; Yuan, Y.-Y.; Zhang, C.-X.; Wang, Q.-L. High Proton Conduction Behavior in 12-Connected 3D Porous Lanthanide–Organic Frameworks and Their Polymer Composites. *CrystEngComm* **2018**, *20*, 3066–3073. [CrossRef]
134. Mukhopadhyay, S.; Das, A.; Jana, T.; Das, S.K. Fabricating a MOF Material with Polybenzimidazole into an Efficient Proton Exchange Membrane. *ACS Appl. Energy Mater.* **2020**, *3*, 7964–7977. [CrossRef]
135. Roshanravan, B.; Younesi, H.; Abdollahi, M.; Rahimnejad, M.; Pyo, S.-H. Application of Proton-Conducting Sulfonated Polysulfone Incorporated MIL-100(Fe) Composite Materials for Polymer-Electrolyte Membrane Microbial Fuel Cells. *J. Clean. Prod.* **2021**, *300*, 126963. [CrossRef]
136. Wang, S.; Luo, H.; Li, X.; Shi, L.; Cheng, B.; Zhuang, X.; Li, Z. Amino Acid-Functionalized Metal Organic Framework with Excellent Proton Conductivity for Proton Exchange Membranes. *Int. J. Hydrogen Energy* **2021**, *46*, 1163–1173. [CrossRef]
137. Li, D.; Li, S.; Zhang, S.; Sun, J.; Wang, L.; Wang, K. Aging State Prediction for Supercapacitors Based on Heuristic Kalman Filter Optimization Extreme Learning Machine. *Energy* **2022**, *250*, 123773. [CrossRef]
138. Ma, T.; Xu, J.; Li, R.; Yao, N.; Yang, Y. Online Short-Term Remaining Useful Life Prediction of Fuel Cell Vehicles Based on Cloud System. *Energies* **2021**, *14*, 2806. [CrossRef]
139. Sun, H.; Sun, J.; Zhao, K.; Wang, L.; Wang, K. Data-Driven ICA-Bi-LSTM-Combined Lithium Battery SOH Estimation. *Math. Probl. Eng.* **2022**, *2022*, 9645892. [CrossRef]
140. Hua, Y.; Wang, N.; Zhao, K. Simultaneous Unknown Input and State Estimation for the Linear System with a Rank-Deficient Distribution Matrix. *Math. Probl. Eng.* **2021**, *2021*, 6693690. [CrossRef]
141. Li, S.; Zhang, Y.; Hu, Y.; Wang, B.; Sun, S.; Yang, X.; He, H. Predicting Metal-Organic Frameworks as Catalysts to Fix Carbon Dioxide to Cyclic Carbonate by Machine Learning. *J. Mater.* **2021**, *7*, 1029–1038. [CrossRef]
142. Zhou, T.; Song, Z.; Sundmacher, K. Big Data Creates New Opportunities for Materials Research: A Review on Methods and Applications of Machine Learning for Materials Design. *Engineering* **2019**, *5*, 1017–1026. [CrossRef]